



International Agreement Report

Implementation of droplet breakup mode in TRACE to improve the prediction of reactor core reflood conditions

Prepared by:

Omar S. Al-Yahia*, Matthew Bernard**, Ivor Clifford*, Grégory Perret*, Stephen Bajorek**, Hakim Ferroukhi*

*Paul Scherrer Institute, Laboratory for Reactor Physics and Thermal-Hydraulics
5232 Villigen PSI
Switzerland

**U.S. Nuclear Regulatory Commission
Washington, DC 20555-0001
USA

K. Tien, NRC Project Manager

**Division of System Analysis
Office of Nuclear Regulatory Research
U.S. Nuclear Regulatory Commission
Washington, DC 20555-0001**

Manuscript Completed: August 2023
Date Published: November 2023

Prepared as part of
The Agreement on Research Participation and Technical Exchange
Under the Thermal-Hydraulic Code Applications and Maintenance Program (CAMP)

**Published by
U.S. Nuclear Regulatory Commission**

AVAILABILITY OF REFERENCE MATERIALS IN NRC PUBLICATIONS

NRC Reference Material

As of November 1999, you may electronically access NUREG-series publications and other NRC records at NRC's Library at www.nrc.gov/reading-rm.html. Publicly released records include, to name a few, NUREG-series publications; *Federal Register* notices; applicant, licensee, and vendor documents and correspondence; NRC correspondence and internal memoranda; bulletins and information notices; inspection and investigative reports; licensee event reports; and Commission papers and their attachments.

NRC publications in the NUREG series, NRC regulations, and Title 10, "Energy," in the *Code of Federal Regulations* may also be purchased from one of these two sources.

1. The Superintendent of Documents

U.S. Government Publishing Office
Washington, DC 20402-0001
Internet: <https://bookstore.gpo.gov/>
Telephone: (202) 512-1800
Fax: (202) 512-2104

2. The National Technical Information Service

5301 Shawnee Road
Alexandria, VA 22312-0002
Internet: <https://www.ntis.gov/>
1-800-553-6847 or, locally, (703) 605-6000

A single copy of each NRC draft report for comment is available free, to the extent of supply, upon written request as follows:

Address: **U.S. Nuclear Regulatory Commission**
Office of Administration
Digital Communications and Administrative
Services Branch
Washington, DC 20555-0001
E-mail: Reproduction.Resource@nrc.gov
Facsimile: (301) 415-2289

Some publications in the NUREG series that are posted at NRC's Web site address www.nrc.gov/reading-rm/doc-collections/nuregs are updated periodically and may differ from the last printed version. Although references to material found on a Web site bear the date the material was accessed, the material available on the date cited may subsequently be removed from the site.

Non-NRC Reference Material

Documents available from public and special technical libraries include all open literature items, such as books, journal articles, transactions, *Federal Register* notices, Federal and State legislation, and congressional reports. Such documents as theses, dissertations, foreign reports and translations, and non-NRC conference proceedings may be purchased from their sponsoring organization.

Copies of industry codes and standards used in a substantive manner in the NRC regulatory process are maintained at—

The NRC Technical Library

Two White Flint North
11545 Rockville Pike
Rockville, MD 20852-2738

These standards are available in the library for reference use by the public. Codes and standards are usually copyrighted and may be purchased from the originating organization or, if they are American National Standards, from—

American National Standards Institute

11 West 42nd Street
New York, NY 10036-8002
Internet: www.ansi.org
(212) 642-4900

Legally binding regulatory requirements are stated only in laws; NRC regulations; licenses, including technical specifications; or orders, not in NUREG-series publications. The views expressed in contractor prepared publications in this series are not necessarily those of the NRC.

The NUREG series comprises (1) technical and administrative reports and books prepared by the staff (NUREG-XXXX) or agency contractors (NUREG/CR-XXXX), (2) proceedings of conferences (NUREG/CP-XXXX), (3) reports resulting from international agreements (NUREG/IA-XXXX), (4) brochures (NUREG/BR-XXXX), and (5) compilations of legal decisions and orders of the Commission and Atomic and Safety Licensing Boards and of Directors' decisions under Section 2.206 of NRC's regulations (NUREG-0750), and (6) Knowledge Management prepared by NRC staff or agency contractors.

DISCLAIMER: This report was prepared under an international cooperative agreement for the exchange of technical information. Neither the U.S. Government nor any agency thereof, nor any employee, makes any warranty, expressed or implied, or assumes any legal liability or responsibility for any third party's use, or the results of such use, of any information, apparatus, product or process disclosed in this publication, or represents that its use by such third party would not infringe privately owned rights.



International Agreement Report

Implementation of droplet breakup mode in TRACE to improve the prediction of reactor core reflood conditions

Prepared by:

Omar S. Al-Yahia*, Matthew Bernard**, Ivor Clifford*, Grégory Perret*, Stephen Bajorek**, Hakim Ferroukhi*

*Paul Scherrer Institute, Laboratory for Reactor Physics and Thermal-Hydraulics
5232 Villigen PSI
Switzerland

**U.S. Nuclear Regulatory Commission
Washington, DC 20555-0001
USA

K. Tien, NRC Project Manager

**Division of System Analysis
Office of Nuclear Regulatory Research
U.S. Nuclear Regulatory Commission
Washington, DC 20555-0001**

Manuscript Completed: August 2023
Date Published: November 2023

Prepared as part of
The Agreement on Research Participation and Technical Exchange
Under the Thermal-Hydraulic Code Applications and Maintenance Program (CAMP)

**Published by
U.S. Nuclear Regulatory Commission**

ABSTRACT

Reflood conditions exhibit complex two-phase flows in fuel assemblies featuring spacer grids. Spacer grids can shatter or split dispersed droplets thereby significantly reducing their diameters, increasing the local heat and mass interfacial transfer, and reducing peak cladding temperature (PCT). The diameter of dispersed droplets downstream of a spacer grid has been shown to be dependent on the Weber number of the incoming droplets and the spacer grid blockage ratio. In this work, a spacer grid droplet breakup model based on the droplet Weber number is implemented into the new three-field version of the U.S. Nuclear Regulatory Commission's TRACE code. The selected droplet break-up model can capture interfacial heat transfer enhancement observed in experimental data and is applicable to both mixing vane and egg-crate style spacer grids. The effect of the droplet breakup model on the three-field version of TRACE is assessed against recent RBHT (Rod Bundle Heat Transfer) experiments, for which TRACE was shown to overpredict the PCT for different initial and boundary conditions. When comparing the predictions of the base capability of TRACE and the three-field code with and without the spacer grid model, the new breakup model reduced the PCT predicted by TRACE by more than 100 K, which resulted in better-predicted PCTs and quenching times for the condition assessed.

TABLE OF CONTENTS

ABSTRACT	iii
TABLE OF CONTENTS.....	v
LIST OF FIGURES.....	vii
LIST OF TABLES	ix
ABBREVIATIONS AND ACRONYMS	xi
1 INTRODUCTION	1
2 SPACER GRID DROPLET BREAKUP MODEL	7
2.1 Implementation of Spacer Grid Droplet Breakup Models	11
3 DESCRIPTION OF RBHT FACILITY	13
4 RBHT TRACE MODEL.....	15
5 RESULTS AND DISCUSSION	19
5.1 Influence of Spacer Grid Droplet Breakup Model.....	19
5.2 Influence of Time Step	27
5.3 Effect of Numerical Solution Method	35
6 CONCLUSION.....	37
7 REFERENCES	39

LIST OF FIGURES

Figure 1-1 Core Reflood Flow Regimes.....	3
Figure 1-2 Influence of Spacer Grid During Reflood Transient.	4
Figure 1-3 Rod Surface Temperature for Test 9021 Of RBHT At 2.9m Elevation with Uncertainty Bands (95% Confidence Intervals) Resulting from The Model Parameter Uncertainty. Uncertainty Bands Are Derived Using Model Parameter Uncertainty That Are Conservative (Labelled Without Calibration) And That Have Been Calibrated Against Similar Experiments (Labelled with Calibration).....	5
Figure 2-1 Schematic Diagram of Droplet Breakup at Spacer Grid.....	7
Figure 3-1 Schematic Diagram Of The RBHT Testing Facility [2].	14
Figure 4-1 Fitting of Initial Boundary Conditions for Test 9005 – Rod Temperature (Left), Vapor Temperature (Middle) And Flow Housing (Right).....	16
Figure 4-2 TRACE Nodalization View of The RBHT Facility.	17
Figure 5-1 Evolution of RBHT Thermal Hydraulic Parameters During Reflood Test - 9005.....	21
Figure 5-2 Evolution of RBHT Thermal Hydraulic Parameters During Reflood Test - 9012.....	22
Figure 5-3 Evolution of RBHT Thermal Hydraulic Parameters During Reflood Test - 9014.....	23
Figure 5-4 Evolution of RBHT Thermal Hydraulic Parameters During Reflood Test - 9015.....	24
Figure 5-5 Evolution of RBHT Thermal Hydraulic Parameters During Reflood Test - 9021.....	25
Figure 5-6 Evolution of RBHT Thermal Hydraulic Parameters During Reflood Test - 9043.....	26
Figure 5-7 RBHT Rod Surface Temperature At 2.695 M For Low Reflood Rate and Low Subcooling Temperature Case (2.5 Cm/S, And 10 K).	28
Figure 5-8 RBHT Rod Surface Temperature At 2.695 M For Low Reflood Rate and High Subcooling Temperature Case (2.5 Cm/S, And 80 K).	28
Figure 5-9 RBHT Rod Surface Temperature At 2.695 M For Medium Reflood Rate and Low Subcooling Temperature Case (5.0 Cm/S, And 10 K).	29
Figure 5-10 RBHT Rod Surface Temperature At 2.695 M For High Reflood Rate and Low Subcooling Temperature Case (15.0 Cm/S, And 10 K).	29
Figure 5-11 RBHT Rod Surface Temperature At 2.695 M For High Reflood Rate and High Subcooling Temperature Case (15.0 Cm/S, And 80 K).	30
Figure 5-12 Influence of Time Step On The Axial Temperature Distribution For Test 9021 (2.5 Cm/S, And 10 K).	31
Figure 5-13 Influence of Time Step On The Axial Temperature Distribution For Test 9029 (2.5 Cm/S, And 47 K).	32

Figure 5-14 Influence of Time Step on The Axial Temperature Distribution For Test 9015 (15.0 Cm/S, And 10 K).....	33
Figure 5-15 Influence of Time Step On The Axial Temperature Distribution For Test 9014 (15.0 Cm/S, And 80 K).....	34
Figure 5-16 The Effect of The Numerical Scheme on The Rod Surface Temperature At 2.695 M For Low Reflood Rate And Low Subcooling Temperature Case (2.5 Cm/S, And 10 K).....	35
Figure 5-17 The Effect of The Numerical Scheme On The Rod Surface Temperature At 2.695 M For Medium Reflood Rate At Low Subcooling Temperature Case (5.0 Cm/S, And 10 K).....	36
Figure 5-18 The Effect of The Numerical Scheme On The Rod Surface Temperature At 2.695 M For High Reflood Rate And High Subcooling Temperature Case (15.0 Cm/S, And 80 K).....	36

LIST OF TABLES

Table 2-1 Definition of Droplet Breakup Model Parameters.....	10
Table 3-1 Boundary Conditions for RBHT Tests.....	14

ABBREVIATIONS AND ACRONYMS

BWR	Boiling Water Reactor
DFFB	Dispersed Flow Film Boiling
ECCS	Emergency Core Cooling System
LB-	Large Break
LOCA	Loss of Coolant Accident
MFB	Minimum Film Boiling
PCT	Peak Cladding Temperature
PWR	Pressurized Water Reactor
RBHT	Rod Bundle Heat Transfer
d_o	Incoming droplet diameter [m]
$d_{s,32}$	Sauter mean diameter [m]
k	Kinetic energy fraction
\dot{m}	Mass flow rate
Nu_f	Nusselt number for interfacial convective heat transfer
Pr_f	Liquid Prandtl number
Re	Reynolds number
U_d	Incoming droplet velocity
We_d	Weber number of the incoming droplet
Y	The dimensionless radiation number
Greek	
ε	Blockage ratio
γ	The liquid mass loss coefficient due to the evaporation of the small droplets
n_l	The number of new generated large droplets
n_s	The number of new generated small droplets
ρ	Density
σ	Surface Tension

1 INTRODUCTION

Several engineering systems experience conditions where two phases are flowing, including heat exchangers, pressurized water reactors (PWRs) during abnormal transients, and boiling water reactors (BWRs) during normal and abnormal operations. In the event of a postulated loss of coolant accident (LOCA) in light water reactors (LWRs), subcooled water is injected into the reactor core through the emergency core cooling system (ECCS) to remove the decay heat, and thus, maintain the peak cladding temperature (PCT) under the regulatory limit (1478 K) [1]. After the onset of water injection, quenching starts from the bottom of the rod bundle and propagates gradually upward to cool the fuel rods. Consequently, the upper region of the rod bundle is expected to undergo the dispersed flow film boiling regime (DFFB). Meanwhile, the PCT will continue to increase until adequate two-phase flow cooling is achieved, and eventually, a reduction in the temperature will occur up until the rod bundle is completely quenched [2]. The increase in the PCT in the post-dryout regime is one of the main safety concerns, which may cause a severe deterioration in the heat transfer, and lead to degradation in the reactor components. Therefore, it is essential to accurately estimate the mass and heat transfer involved in the DFFB regime. To enhance the accuracy of transient behavior calculations in nuclear power plants, thermal hydraulic system analysis codes, such as US-NRC TRACE, are continually improved. These improvements involve solving the three field equations, using an advanced numerical solving technique, and selecting correlations and closure modules associated with complex two-phase phenomena. Code prediction accuracy is highly dependent on the complexity of thermal hydraulic phenomena and geometrical parameters. For example, during a nuclear reactor reflood transient, all heat transfer and flow regimes are expected to occur through the heated tube bundle in the core region [3], as illustrated in Figure 1-1, which can reduce the accuracy to predict the peak cladding temperatures (PCT) and/or quenching time during reflood phase, especially with the presence of spacer grids. Accordingly, it is important to have a clear understanding of the thermal-hydraulic response during the reflood phase of the accident to ensure that the cladding temperature is always below the allowable safety limit [4]. The PCT occurs in the dispersed flow boiling region, where the dispersed liquid droplets exist within the continuous vapor flow region. These dispersed droplets have a large surface area-to-volume ratio, providing a significant interfacial area for heat and mass transfer, which leads to a reduction in the PCT. This enhancement in the cooling rate is highly proportional to the droplet size that determines the interfacial heat transfer area between the dispersed droplets and continuous vapor [4].

The US-NRC TRACE code is a best-estimate thermal hydraulic system code. It has several models and correlations that are applicable to different transients including large break loss of coolant accident (LBLOCA). However, the complexity of the reflood transient reduces the accuracy of predicting the thermal hydraulic parameters during the reflood. There are specific models in the TRACE code that can be used to predict thermal hydraulic phenomena during the reflood transient [5]. However, during the OECD/NEA RBHT project, several thermal hydraulic codes, including TRACE, over-predicted the temperature of the rod surface, and the prediction of the quench front of the rod bundle diverged from experimental results [6]. This was also observed during simulations of ABB Atom and FLECHT-SEASET reflooding tests [7, 8]. As a result, an extensive investigation of the RBHT experimental data showed that the spacer grid has a significant impact on heat and mass transfer through the rod bundle. As illustrated in Figure 1-2, the temperature downstream the spacer grids are less than the ones upstream, although the quenching time is delayed downstream. The TRACE code has specialized models that can take into account the effect of spacer grids, such as an increase in pressure drop, enhancement of single-phase heat transfer, and a spacer grid rewet model [5]. However, despite these models,

TRACE could not reproduce the trend observed. During the RBHT project, TRACE simulations were performed with several code versions and assessing the impact of the uncertainty of the model parameters having a significant sensibility in the context of reflood experiments [9]. Figure 1-3 shows an example of rod surface temperature predicted with TRACE considering the 95% confidence intervals resulting from the propagation of the model parameter uncertainty with and without calibration against similar reflood experiments. Even when the probability distribution of the model parameters have been conservatively assessed, i.e., without calibration, the uncertainty bands do not comprise the experimental temperature profile. The TRACE models are therefore inadequate to capture the physics displayed in such reflood experiments.

The commercial nuclear reactors such as BWRs and PWRs use spacer grids along the fuel rod assemblies to maintain a fixed pitch between the rods, which prevent any damages caused by vibration from fluid flow and ensure a secure passage for the flow. Mixing vanes are added to spacers to produce cross-flows and vortices that enhance turbulent mixing and local heat transfer. Spacer grids can shatter or split the incoming dispersed droplets thereby significantly reducing their diameters and enlarge the interfacial area, increasing the local heat and mass interfacial transfer, and thus reducing peak cladding temperature (PCT). In reflood tests conducted on a 6x6 heated rod bundle, Sugimoto and Urao [10] observed significant droplet breakup when the droplets collided with grid spacer straps. The downstream droplet diameter decreased as the grid blockage ratio increased. The effectiveness of spacer grid in shattering the incoming droplet is enhanced with larger droplet diameters [11, 12]. Therefore, significant droplet breakup can occur when droplets with a high Weber number (determined by droplet diameter, density, velocity, and surface tension) collide with spacer grid straps. Hence, new droplets with a smaller Sauter diameter and larger number density are generated. This increases the interfacial heat transfer area downstream of the spacer grid and accelerates the flow, while simultaneously cooling the rods downstream of the spacer grid by rapidly evaporating the shattered droplets [13].

Over the past few decades, the interfacial heat and mass transfer behavior of the droplet field entrained in continuous vapor field has been extensively investigated. In the presence of spacer grids, the droplets will contact the dry and wet surface of the spacer grid at different angles [2]. Many researchers have been interested to investigate the droplet breakup upon collision with a spacer grids and its influence on the PCT during the reflood [4, 14]. In 1966, Wachters and Westerling [15] conducted an experimental study to investigate the influence of Weber number on the droplet breakup, and they observed that the droplet breakup occurs when the Weber number of the incoming droplets exceeded 80. Droplet Weber number represents the ratio of the droplet inertia to its surface tension. Thus, the velocity of incoming droplets have a significant impact on droplet heat transfer [16]. Hamdan et al. [17] carried out an experimental study to investigate the droplet behavior impacting on a hot surface above the minimum film boiling (MFB) temperature. They observed that the droplets did not breakup if the Weber number was less than 30. However, for larger Weber number droplets, the incoming droplets will breakup into several micro-size droplets and a larger size droplet that has a diameter smaller than the original incoming droplet. Several empirical correlations were developed to estimate the shattered droplet diameter as a function of Weber number, spacer grid blockage ratio [18], and the incoming droplet diameter to strip thickness of the spacer grid [19]. In 1977, Paddock [20] used photography to observe droplet behavior and noted an increase in the number of droplets downstream of the grid spacer due to droplet breakup. Rane and Yao [21] demonstrated that droplets in a dispersed two-phase flow regime could serve as a distributed heat sink in the continuous vapor phase region. Senda [22] investigated the interaction of droplets with heated flat plates and observed that a high Weber numbers could cause droplets to flatten into liquid sheets before fragmenting into smaller droplets. In 1998, Koszela [23] carried out experimental study using 3×3 rod bundle to investigate the influence of spacer grids design on the reflood heat transfer. He observed that using mixing vane

spacer grids significantly reduces the PCT at low reflood rate, and reduces the heat transfer for the post-CHF (critical heat flux) regime at high reflood rates. The same findings for the effects of spacer grids type on heat transfer enhancement in a rod bundle were observed experimentally and numerically by Cho et al. [24] and In et al. [25], respectively.

Droplet breakup in the DFFB regime significantly enhances the cooling performance during the reflood process. To quantify the amount of cooling enhancement, it is necessary to determine the Sauter-mean-diameter ratio of the droplets downstream and upstream of the grid. Cheung and Bajorek [4] developed a model to predict the new droplets Sauter diameter downstream of the wet spacer grid. Recently, Jin et al. [2] extended Cheung and Bajorek's [4] research work to predict the droplet breakup for the dry spacer grid. They determined the relationship between the Sauter-mean-diameter ratio and the controlling parameters of the dispersed flow-grid spacer system. Their model was validated against the RBHT experimental data. Accordingly, in the present study, Cheung and Bajorek [4] and Jin et al. [2] droplet breakup models for the wet and dry spacer grid, respectively, have been implemented into the nuclear thermal hydraulic system analysis code TRACE. The implementation has been made in TRACE code to obtain more reasonable predictions for reflood peak clad temperatures (PCTs) and quenching times. The spacer grid droplet breakup models based on the energy and mass balance and the droplet Weber number are implemented into the newly developed three-field version of the U.S. Nuclear Regulatory Commission's TRACE code. The effect of the droplet breakup model on the three-field version of TRACE is assessed against the recent RBHT experiments, for which TRACE was previously shown to overpredict the rod surface temperature and PCT for different initial and boundary conditions. Moreover, a sensitivity study was performed in order to examine the influence of time step on the prediction of rod surface temperature during the reflood process. The report consists of six sections. The first section is the introduction including the literature review about the importance of droplet breakup on the heat and mass transfer during reflood. The second section is discussing the spacer grid droplet breakup model and its implementation into the three-field TRACE code. Section 3 includes the description of the RBHT testing facility. TRACE model of the RBHT facility is described in section four. Section 5 is discussing the validation results of the spacer grid breakup model against the RBHT experimental data. Finally, section six includes the conclusion of this research work.

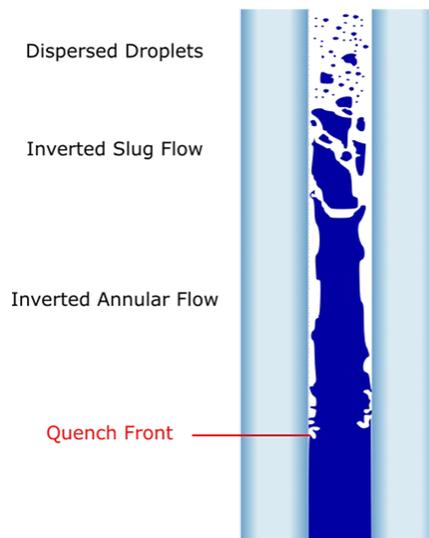


Figure 1-1 Core Reflood Flow Regimes.

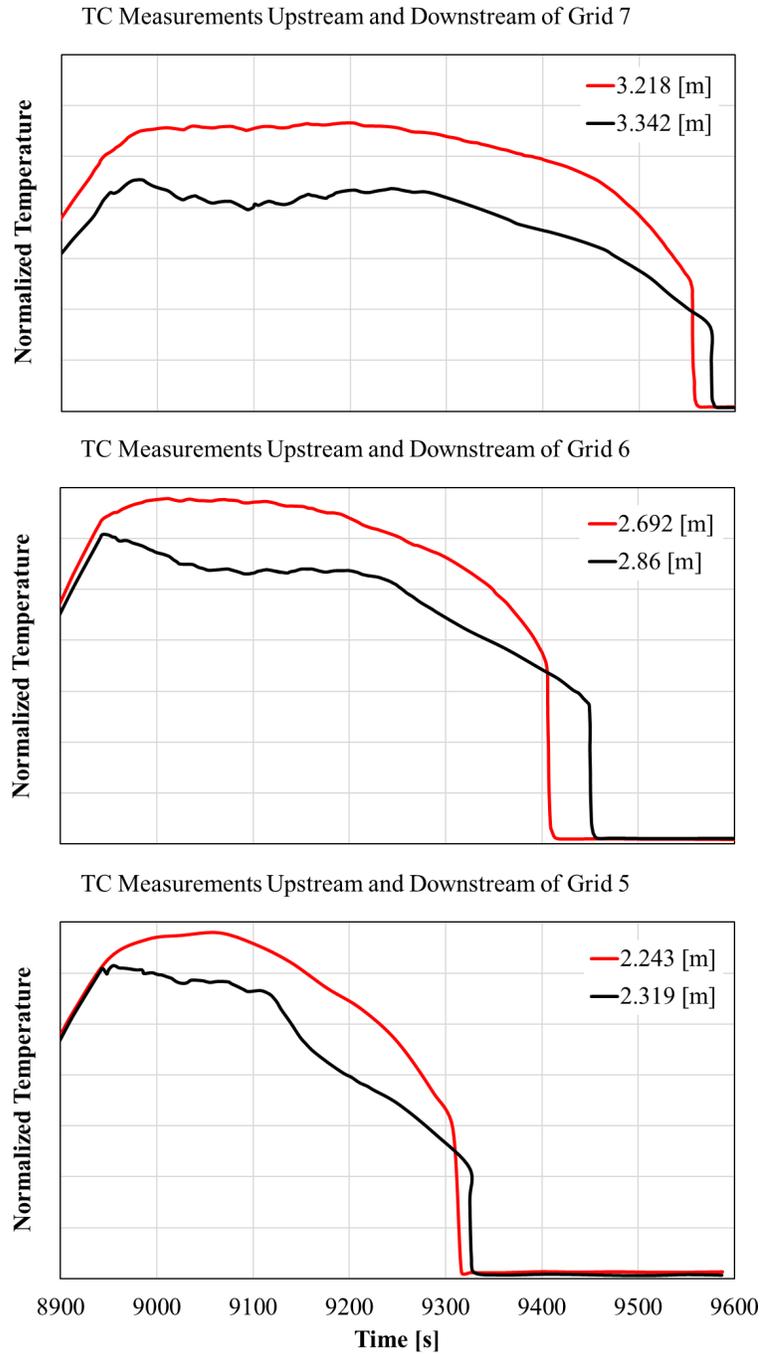


Figure 1-2 Influence of Spacer Grid During Reflood Transient.

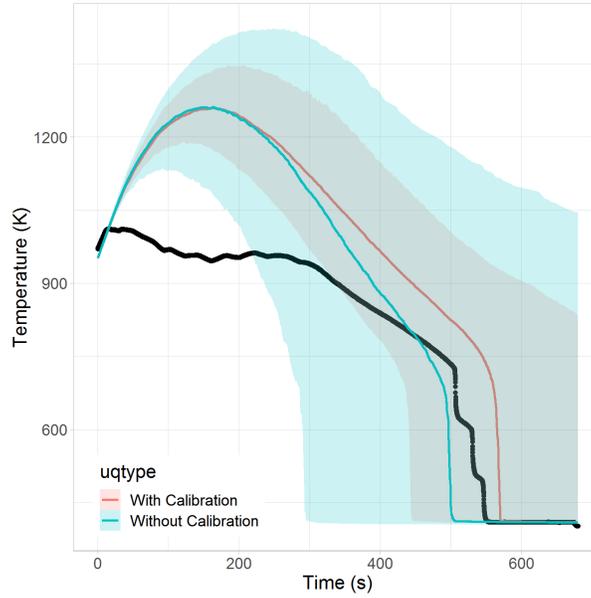


Figure 1-3 Rod Surface Temperature for Test 9021 Of RBHT At 2.9m Elevation with Uncertainty Bands (95% Confidence Intervals) Resulting from The Model Parameter Uncertainty. Uncertainty Bands Are Derived Using Model Parameter Uncertainty That Are Conservative (Labelled Without Calibration) And That Have Been Calibrated Against Similar Experiments (Labelled with Calibration).

2 SPACER GRID DROPLET BREAKUP MODEL

Spacer grids have a significant influence on the fuel assembly thermal hydraulic behavior during normal and abnormal conditions [23, 24, 26, 27]. During reflood, the DFFB regime occurs, and the heat is transferred via several mechanism including convection between the heating surface and vapor phase, interfacial convection between vapor and liquid droplets, radiation heat transfer between the heating surface and the vapor/droplets, and direct heat transfer between the heating surface and liquid droplets. On the other hand, spacer grids have a considerable effect on the dispersed droplets flow through the rod bundle. The dispersed droplets can collide with the straps of the spacer grids, which shatters the droplets into several small diameter droplets. Introducing new smaller droplets results in larger interfacial area for heat and mass transfer at the downstream of the spacer grids, which leads to increased heat removal from the heated surface and superheated vapor. Figure 2-1 illustrates the breakup process of incoming droplet collides with the spacer grid. Generally, the incoming droplets split into two groups of droplet diameters: a group of large droplets with a similar diameter of the incoming droplets, and a group of significantly smaller diameter droplets [19].

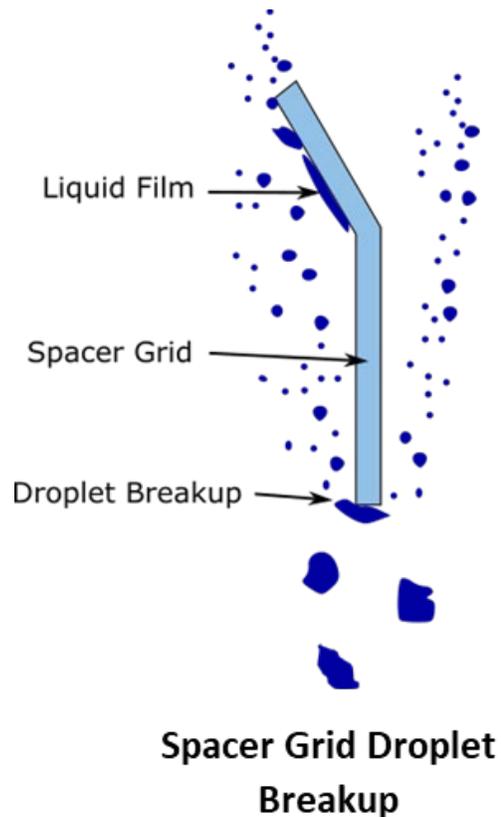


Figure 2-1 Schematic Diagram of Droplet Breakup at Spacer Grid.

Several researchers proposed empirical correlations to estimate the Sauter mean diameter of the secondary droplets. Yao et al. [19] performed experimental study to investigate the water droplet breakup phenomenon. The diameter of dispersed droplets downstream of a dry spacer grid has been shown to depend on the Weber number of the incoming droplets and the spacer grid blockage ratio [19, 28]. The authors estimated the Sauter mean diameter of the new droplets as:

$$\frac{d_{s,32}}{d_o} = A We_d^{-B} \quad (1)$$

where We_d is the Weber number of the incoming droplet and where Yao et al. [19] proposed to make A and B functions of the incoming droplet diameter and the width of spacer strap, while Paik et al. [18] used constant values for A and B of 6.16 and 0.53, respectively. The Weber number is defined as the ratio of droplet inertia to the surface tension, as expressed in Eq. 2. Thus, the droplets must have sufficient inertial forces ($We_d > We_{crit}$) to experience the breakup.

$$We_d = \frac{\rho_d U_d^2 d_o}{\sigma} \quad (2)$$

Akhtar and Yule [29] performed an experimental study for high Weber number droplets impacting on a heated surface. They proposed the following empirical correlation to estimate the Sauter mean diameter of the secondary droplets

$$\frac{d_{s,32}}{d_o} = 0.2 + \left(\frac{60}{We_d}\right)^a \quad 1.0 < a < 1.5 \quad (3)$$

Hamdan et al. [17] et al. compared their experimental results against Yao et al. [19] model, which has been implemented into COBRA-TF code, and the model over-predicted their experimental results. Thus, they proposed new modified droplet breakup model for droplet having We_d larger than 30, as

$$\frac{d_{s,32}}{d_o} = (1.25 - 2.9 \exp(-0.09 We_d)) \left(We_d^{0.8} \exp\left(\frac{-78}{We_d}\right) \right)^{-1/3} \quad (4)$$

The aforementioned models are simple models to estimate the droplet breakup. However, Jin et al. [2] illustrated that Yao et al. [19], Lee et al. [28], and Paik et al. [18] models underpredicted the

RBHT experimental data for dry spacer grids. The authors extended the original work of Cheung and Bajorek [4] to enhance the droplet breakup model for the dry spacer grid based on the RBHT experimental data. In their model, the droplet breakup is depending on the Weber number, the blockage ratio of spacer grid, kinetic energy and Reynold number of incoming droplets, interfacial heat transfer, non-dimensional radiation number, distance from the initial breakup point, and liquid mass loss coefficient due to the evaporation of the small droplets. Accordingly, the Sauter mean diameter of the new droplets downstream of the dry spacer grid can be expressed as:

$$\frac{d_{32}}{d_o} = \frac{1 - \gamma \epsilon n_s \frac{d_s^3}{d_o^3}}{1 - \gamma \epsilon n_s \frac{d_s^2}{d_o^2} + \frac{\epsilon k W e_d}{12}} \quad (5)$$

All parameters of Eq. 5 are defined in Table 2-1. The selected droplet break-up model can capture interfacial heat transfer enhancement observed in experimental data and is applicable to both mixing vane and egg-crate style spacer grids. The spacer grids only partially block the core flow area, and many of the incoming droplets pass through the spacer grid without any contact with the spacer strap. Thus, the number of droplets colliding with the spacer grid is directly proportional to the spacer grid blockage ratio and among these droplets about 60% will breakup [2]. Hence, the mass flowrate of the new small droplets (\dot{m}_s) and unaffected large droplets (\dot{m}_l) downstream of the spacer grids can be estimated using Eq. 3 and Eq. 4, respectively.

$$\dot{m}_s = 0.6\epsilon \times \dot{m}_o \quad (6)$$

$$\dot{m}_l = \dot{m}_o - \dot{m}_s \quad (7)$$

where ϵ is the total blockage ratio of the spacer grid and \dot{m}_o is the mass flow rate upstream.

Table 2-1 Definition of Droplet Breakup Model Parameters.

Breakup model parameters	Definition
$k = 2.164We_d^{-0.442}$	Kinetic energy fraction of the incoming droplet that is converted to surface energy of the new generated droplets
$n_s = \frac{n_l d_l^3 d_o^3}{c d_o^3 d_s^3}$	The number of new generated small droplets
$n_l = 1 \sim 2$	The number of new generated large droplets
$\frac{d_s}{d_o} = \left[\left(\frac{kWe_o}{12} + 1 - n_l \frac{d_l^2}{d_o^2} \right) / \left(\frac{n_l d_l^3}{c d_o^3} \right) \right]^{-1}$	The ratio of new small group Sauter diameter to the incoming droplet Sauter diameter
$\frac{d_l}{d_o} = \left(\frac{c}{(1+c)n_l} \right)^{\frac{1}{3}}$	The ratio of new large group Sauter diameter to the incoming droplet Sauter diameter
$C = \frac{F_l}{1-F_l}$	The volume ratio of the large droplet group to small droplet group
$F_l = \left(0.0042 \left(\frac{d_o}{W} \right) - 0.0386 \right) \ln We_d + 1.04$	The volume fraction of large droplet groups to the original droplet volume
$\gamma = 0.55 \left(\left(\frac{Nu_f Ja_f}{Pr_f Re_d} + Y \right) \left(\frac{L}{d_s} \right) \right)^{0.27}$	The liquid mass loss coefficient due to the evaporation of the small droplets
$Y = \frac{\epsilon_r \sigma (T_w^4 - T_d^4)}{h_{fg} \rho_d u_d}$	The dimensionless radiation number
$Nu_f = (2 + 0.57 Re_v^{0.5} Pr_f^{0.33}) (1 + B_f)^{-0.7}$	Nusselt number for interfacial convective heat transfer
$Re_v = \frac{\rho_v u_r d_s}{\mu_v}$	Vapor Reynolds number
$Pr_f = \frac{c_p \mu_f}{k_f}$	Liquid Prandtl number
$B_f = Ja_f = \frac{c_p (T_v - T_d)}{h_{fg}}$	Mass transfer number
$Re_d = \frac{\rho_d u_d d_s}{\mu_v}$	Droplet Reynolds number

2.1 Implementation of Spacer Grid Droplet Breakup Models

The US-NRC TRACE code has specialized models that account for the presence of spacer grids in the fuel assembly, such as the increase in the pressure drop, enhancement in the single-phase heat transfer, and the rewetting of the spacer grid. However, the spacer grid droplet breakup is the crucial factor during the reflood transient. TRACE version 5 patch 7 does not have droplet breakup model, and the droplet field is evaluation of an empirical correlation based on the local flow conditions. The correlations determine the mass fraction of liquid flowing as entrained droplets during annular/mist flow regime [5], and the droplet diameter is determined using empirical formula as a function of the liquid film Reynolds number. Therefore, implementing the droplet breakup model into TRACE v5p7 will not be sufficient to consider the influence of the droplet breakup downstream the spacer grids. Nevertheless, the droplet field within the new three-fields TRACE is modeled with the mass, momentum, and interfacial area density equations. Thus, the droplet diameter is a fundamental parameter that obtained from the interfacial area transport. TRACE three-field takes into account the pool and liquid film entrainment models, without consideration to the droplet breakup. In this study, Jin et al. [2] droplet breakup model and Yao et al. [19] droplet breakup model have been implemented into US-NRC three-fields TRACE code for dry and wet spacer grids, respectively. The net breakup parameters are the entrained mass and interfacial area, which are added to the source terms for the net entrainment parameters. The droplet breakup has the largest impact of the reflood cooling performance.

3 DESCRIPTION OF RBHT FACILITY

RBHT is a separate effect test facility located at US-Pennsylvania State University, which was constructed to investigate the reflood transient through rod bundle with spacer grid. The RBHT facility consists of a 4-m high stainless steel test section, which contains a 7 × 7 rod bundle, a lower and an upper plenum, injection pump, steam separator, pressure oscillation damping tank, boiler, and liquid carryover tanks, as shown in Figure 3-1. The rod bundle models a part of the typical Pressurized Water Reactor (PWR) fuel assembly, in which the rod diameter is 9.49 mm and rod pitch is 12.59 mm. 45 rods are heated electrically with triangular axial power shape. The power peak is 150 % of the average power at an elevation of 2.74 m. The other four rods that are located at the corners are not heated. The total heated length of the rod bundle is 3660 mm. The test section is surrounded by Inconel 600 square flow housing, with six transparent windows to visualize the two-phase and droplet behavior through the bundle. Additionally, the test section contains seven mixing vane spacer grids [2, 30].

RBHT facility is well instrumented (512 data channels) to measure the important transient reflood parameters. Numerous temperature (256 TCs) and pressure sensors (23) are distributed inside the test section to measure the rod surface temperatures, bulk temperature, and pressure drop, as well as, high speed camera to estimate the bubble and droplet size. All these measurement are important to investigate the quenching behavior during reflood. Two carryover tanks (small and large) are used to measure the fraction of liquid carried over during the reflood. A more detailed description of the RBHT facility can be found in [31-33].

Before the start of the test, the rod bundle is heated to a specific peak cladding temperature larger than Leidenfrost point to simulate the accident scenarios in LWRs. After that, subcooled water at various temperature and mass flow rates is injected through the lower plenum to quench the rod bundle. Meanwhile, a significant amount of droplets are generating while the quench front is moving upward the rod bundle. A large number of RBHT tests were performed under various initial and boundary conditions (i.e., inlet temperature, inlet flow velocity, operation pressure, and heating power). Recently, within the framework of the OECD/NEA RBHT project (2020-2022) [34], eleven open phase tests have been provided to the project partners to assess the performances of different system thermal hydraulic codes. Table 3-1 summarizes the boundary conditions of the 11 OECD/NEA RBHT tests.

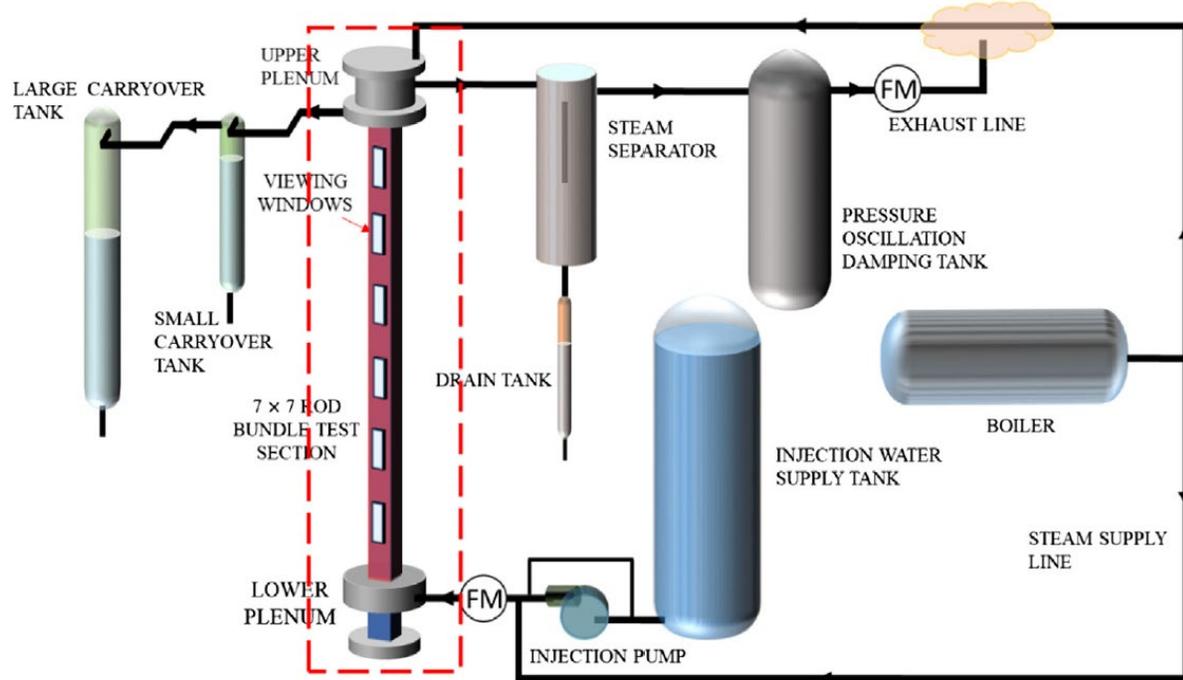


Figure 3-1 Schematic Diagram Of The RBHT Testing Facility [2].

Table 3-1 Boundary Conditions for RBHT Tests.

Test	Reflow rate (cm/s)	Reflow inlet subcooling (K)	Bundle power (kW)
9005	5	14	144
9011	Step (8, 5, 3, 1.2)	26	144
9012	Varying (± 2.5)	9	144
9014	15	80	252
9015	15	12	252
9021	2.5	10	144
9026	2.5	79	144
9027	2.5	32	144
9029	2.5	48	222 (Decay)
9037	5	11	144
9043	0.5	2.8	35

4 RBHT TRACE MODEL

RBHT tests have been extensively utilized to validate the US-NRC thermal hydraulics code TRACE [9, 31-33]. The RBHT model used in the paper is based on that referenced as 'Trace-v5p5' in [9]. In this report, the simulations were performed using the same TRACE model for the RBHT facility but with TRACE version 5 patch 7 (v5p7) and the newly developed 3-field TRACE with and without the droplet breakup model. The model consists of various thermal hydraulic and heat structure components, as shown in Figure 4-2. The test section is represented as a 3D Cartesian VESSEL component with 32, 2, and 1 cells in the axial, Y, and X directions, respectively. Axial cells have a height between 11cm and 15cm, except for the first 10 cm where it is subdivided in two and above 3.4 m where it is approximately 9 cm. The two transverse cells (Y) represent the flow around the inner (25 heated rods) and the outer (20 heated and 4 structural rods) groups of rods. We distinguish between these two groups because they experience slightly different flow conditions due to the wall effects from the flow housing. The heated and unheated rods are modelled using heat structure components with 30 axial cells. The test section walls are similarly modelled using heat structure components with 32 axial cells.

The heated rods (HTSTR6 and 16) have 30 axial cells and 9 radial nodes (8 intervals), with the liquid level tracking, axial conduction, and fine mesh reflood model enabled. Since there is no heating in the top two cells of the VESSEL, only 30 axial cells are included in the rod heat structures. A POWER component provides the power distribution in the heated rods. The flow housing (HTSTR7) has 32 axial cells and 3 radial nodes, with axial conduction enabled. However, there are no fine meshes, and the liquid level tracking and reflood model are not enabled. This heat structure is not powered, and heat loss from the outer surface of the flow housing is neglected. The heat structure for the structural corner rods (HTSTR9) includes 30 axial cells and 5 radial nodes, with axial conduction and liquid level tracking enabled. However, there are no fine meshes, and the reflood model is not enabled. This heat structure is not powered. No external heat loss is considered.

As illustrated in Figure 4-2, two FILL and two BREAK components are linked to two pipes that are connected to the inlet and outlet region of the VESSEL component, respectively. The hydraulic diameter and flow area of the pipes match those of the inner and outer regions of the vessel. The BREAK components have an initial pressure and mixture temperature determined from the experimental system pressure. The FILL components have the same initial pressure and temperature determined from the experimental subcooling temperature.

The initial and boundary conditions are based on the experimental test conditions. The model was pre-conditioned with the initial conditions obtained from experimental data when the water injection began, 10 seconds before the transient started. This pre-conditioning period allowed the simulation to stabilize before the transient was initiated. The initial conditions included the temperature of the vapor in the test section, as well as the temperatures of the shroud and rod groups, which were classified as inner rods (5x5 central bundle), outer rods (20 heated rods in periphery), and structural rods (4 non-heated corner rods). The initial temperature profiles are derived from experimental thermocouple measurements immediately before the start of reflood and interpolated (see e.g., Figure 4-1 for test 9005).

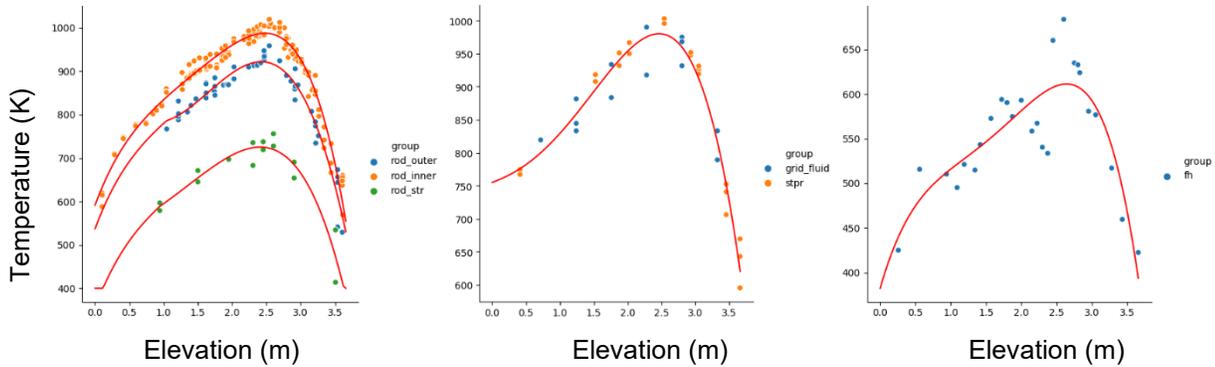


Figure 4-1 Fitting of Initial Boundary Conditions for Test 9005 – Rod Temperature (Left), Vapor Temperature (Middle) And Flow Housing (Right).

The following sensitivity tests to the nodalization and code version were conducted during the development of the reference TRACE model.

1. The radial nodalization of the test section – either a VESSEL or 1D PIPE component;
2. The axial nodalization of the test section – the number of axial nodes was varied between 16 and 64;
3. The modelling of the feed and exit lines – either 2 PIPES, a PIPE, a VESSEL Junction or PLENUM component;
4. The effect of the heat losses through the test section wall;
5. The effect of thermal radiation in the test section;
6. The effect of TRACE code version – TRACE v5 patches 3, 5 and 7.

While differences were observed between the cases considered, these were generally smaller than error between the code prediction and the experimental data. The reference nodalization of Figure 4-2 was chosen since it represents a good balance between performance and accuracy. For the three TRACE versions, the stability enhancing two steps (SETS) method was selected (NOSETS=0) with 0.003 seconds as a maximum time step.

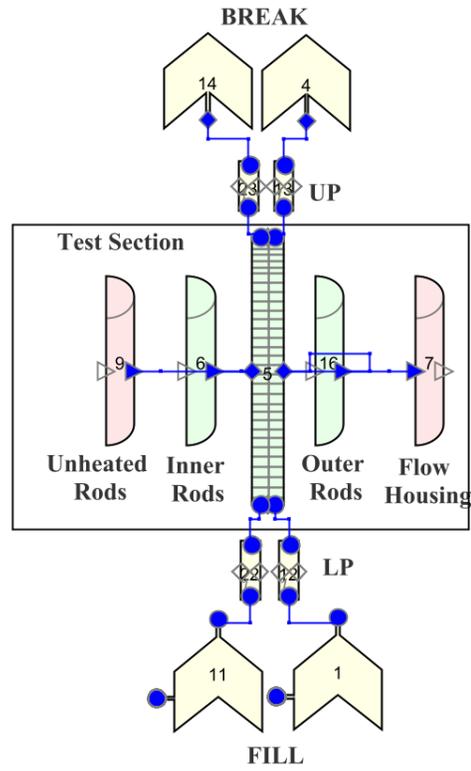


Figure 4-2 TRACE Nodalization View of The RBHT Facility.

5 RESULTS AND DISCUSSION

5.1 Influence of Spacer Grid Droplet Breakup Model

In general, the spacer grids have a significant influence on the flow behavior inside the fuel assembly, especially for the two-phase flow regimes. In this section, we discuss the influence of spacer grid droplet breakup model on the prediction of reflood phenomena. Thus, the predicted results from TRACE v5p7, 3-field TRACE without droplet breakup (3F), and 3-field TRACE with droplet breakup (3F-DB) are compared against the RBHT experimental data. The same TRACE model of RBHT test facility was used for all tests. The initial boundary conditions were extracted from the experimental data at the start of the test. The results of some selected tests are shown in Figure 5-1 to Figure 5-6.

Starting with test 9005 that has inlet velocity of 5 cm/s, inlet subcooling of 10 K, and peak power of 1.31 kW/m, the overall trend of the rod surface temperature at two different axial locations (2.695 m and 2.885 m from the inlet) is similar for the three simulations. However, the maximum rod surface temperature and quenching time are different, as illustrated in Figure 5-1. The rod surface temperatures before quenching are overpredicted with TRACE v5p7 and TRACE 3F, and better predicted by TRACE 3F-DB. Consistent with the experimental data, the surface temperature of the rod decreases rapidly at the beginning of the test in TRACE 3F-DB. However, in TRACE v5p7 and 3F simulations, temperatures initially rise for the first 50 seconds before gradually decreasing over time. The differences observed in the calculations are primarily attributed to the droplet field and droplet breakup models, which enhance interfacial heat and mass transfer. Additionally, the simulations indicate earlier quenching of the rods than in the experiments. Notably, both TRACE 3F and 3F-DB provide more accurate quenching time estimates than TRACE v5p7, with a difference of approximately 50 seconds. However, the liquid carryover fraction is overpredicted after about 25 seconds from the start of the test. In contrast, TRACE v5p7 and 3F-DB offer slightly better estimates of liquid carryover during the first 100 seconds. Furthermore, the total pressure drop is overestimated for the first 150 seconds, followed by underestimation. This trend is influenced by the average void fraction and quench elevation.

During Test 9012, a low inlet subcooling and oscillatory flooding rate test was conducted. The flooding rate has a sinusoidal pattern with an average velocity of 2.5 cm/sec. The mean velocity experienced oscillations of ± 2.5 cm/sec, leading to flooding rates ranging from approximately 0 cm/sec to 5 cm/sec. The inlet subcooling is 9 K. However, in the simulations, TRACE's predictions for the quench time throughout the bundle are overestimated. The peak cladding temperature is also significantly overestimated by TRACE v5p7 and TRACE 3F. TRACE 3F-DB shows better estimation for the rod surface temperature, as presented in Figure 5-2. Moreover, TRACE's predictions for the carryover fraction are overestimated.

Tests 9014 and 9015 share a similar inlet velocity of approximately 15 cm/s, peak power of 2.30 kW/s, and inlet subcooling temperature of 80 K and 11.7 K, respectively. As depicted in Figure 5-3 and Figure 5-4, the transient is faster in test 9014 due to its lower inlet temperature. Using TRACE 3F-DB, the rod surface temperature is well predicted at various axial locations for both tests, primarily influenced by the droplet breakup model. Following the test initiation, TRACE 3F-DB captures the immediate reduction in the rod surface temperature. However, a comparable overprediction of the maximum rod temperature is observed for both TRACE v5p7 and TRACE 3F. The liquid carryover of three TRACE versions exhibits overprediction in compare with the

experimental data. Additionally, the prediction of the quenching front and pressure drop agree well with the experimental results for test 9014. However, for test 9015, the calculated quenching occurs earlier than the experimental result.

As shown in Figure 5-5, the trend described above is repeated in test 9021, which features a lower reflood rate with an inlet velocity of 2.5 cm/s and the same peak power as test 9005. Due to the reduced reflood rate, the quenching is delayed. In test 9021, the deviation of TRACE v5p7 results from the experimental data is more pronounced. However, the rod surface temperatures at 2.695 m and 2.885 m are well predicted by TRACE 3F-DB. Regarding the quenching time, both TRACE 3F and 3F-DB offer accurate predictions, whereas TRACE v5p7 quenches approximately 150 seconds earlier along the entire test section. Furthermore, at the upper location of the test section, the quenching is delayed according to the calculations obtained from TRACE 3F and 3F-DB, and it does not occur near the outlet. Moreover, all TRACE versions over-predict the liquid carryover fraction.

Figure 5-6 presents the experimental and calculated results of test 9043, which is a very low reflood rate case with an inlet velocity of 0.5 cm/s and a peak power of 0.32 kW/m. Through the first half of the test section, the quenching front is well estimated by the three simulations, and it is about 20 seconds delayed in the upper region of the test section. This explains why TRACE slightly underestimates the pressure drop at the later stages of the test. During the first 600 seconds, the rod surface temperature increases gradually up to 20% higher than the initial temperature, and then reduces gradually until the rod bundle is quenched. In all TRACE calculations, the maximum rod surface temperature is around 20% higher than the experimental value at 2.695 m and 10 % at 2.885 m, as illustrated in Fig. 6. The figure shows that the calculated rod surface temperature is similar for the three TRACE versions, which conclude that the droplet field has a minor effect during the very low reflood rate, and/or the generated droplets are small enough that cannot be captured with the current single group droplet field model.

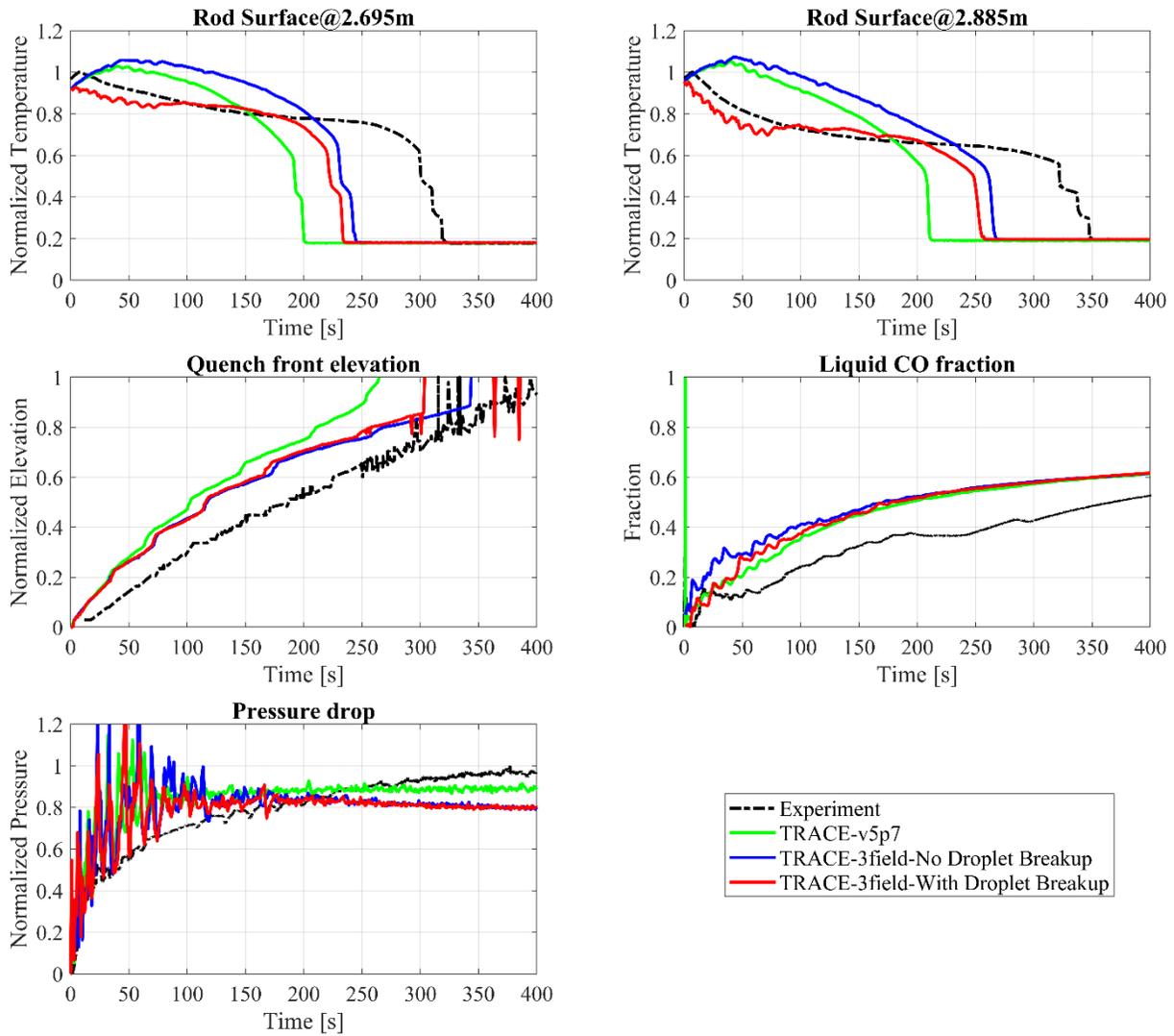


Figure 5-1 Evolution of RBHT Thermal Hydraulic Parameters During Reflood Test -9005.

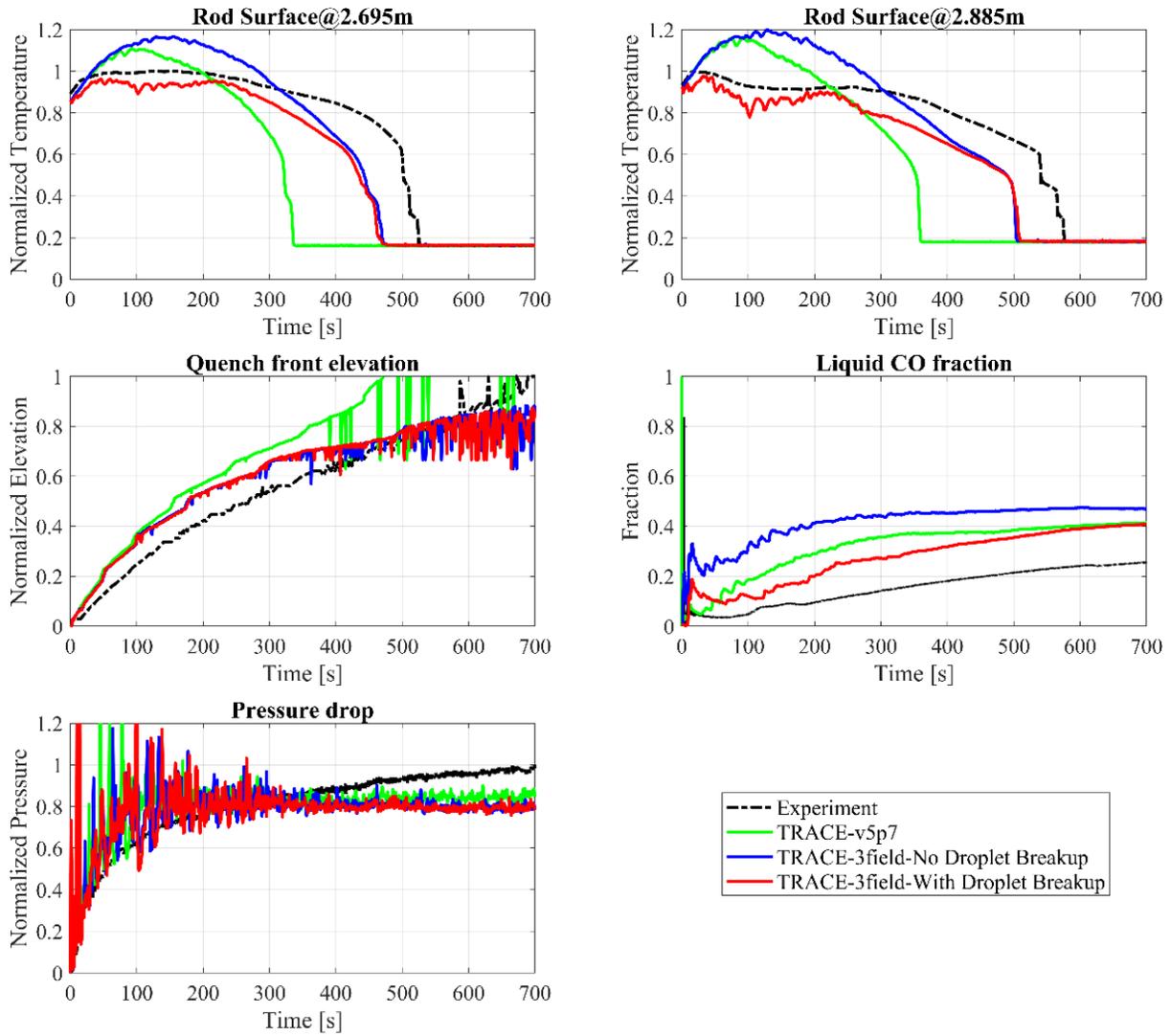


Figure 5-2 Evolution of RBHT Thermal Hydraulic Parameters During Reflood Test -9012.

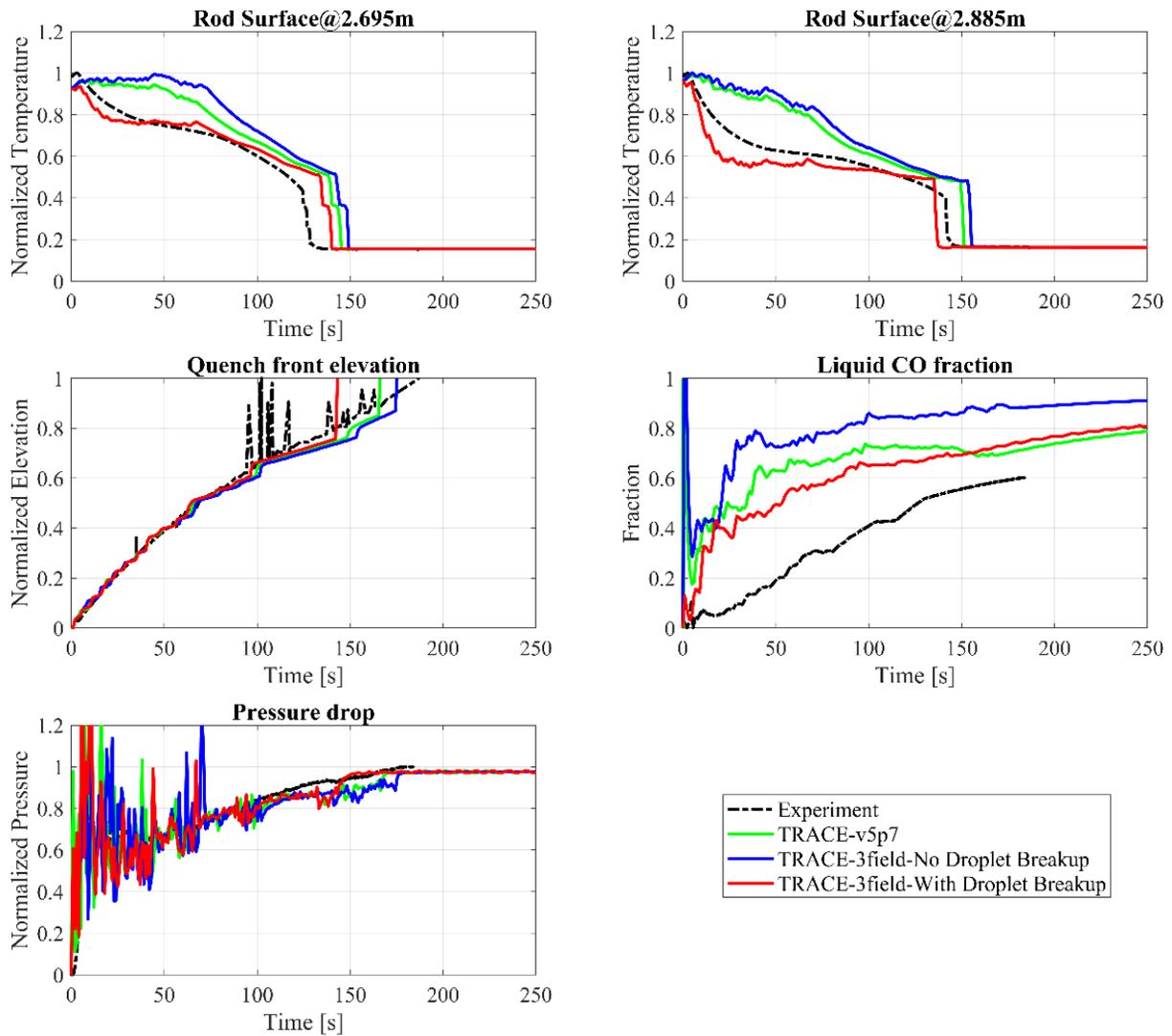


Figure 5-3 Evolution of RBHT Thermal Hydraulic Parameters During Reflood Test -9014.

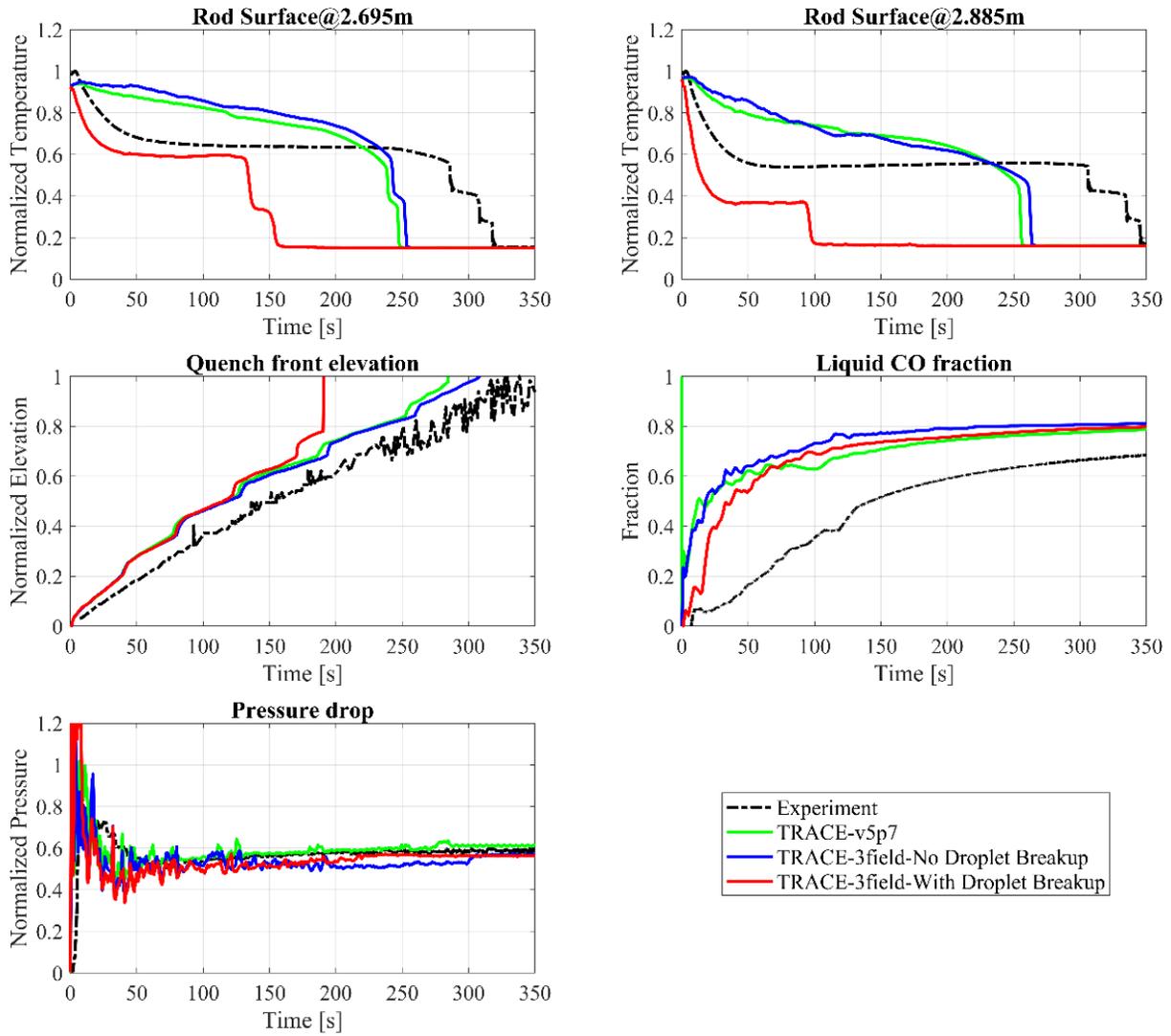


Figure 5-4 Evolution of RBHT Thermal Hydraulic Parameters During Reflood Test -9015.

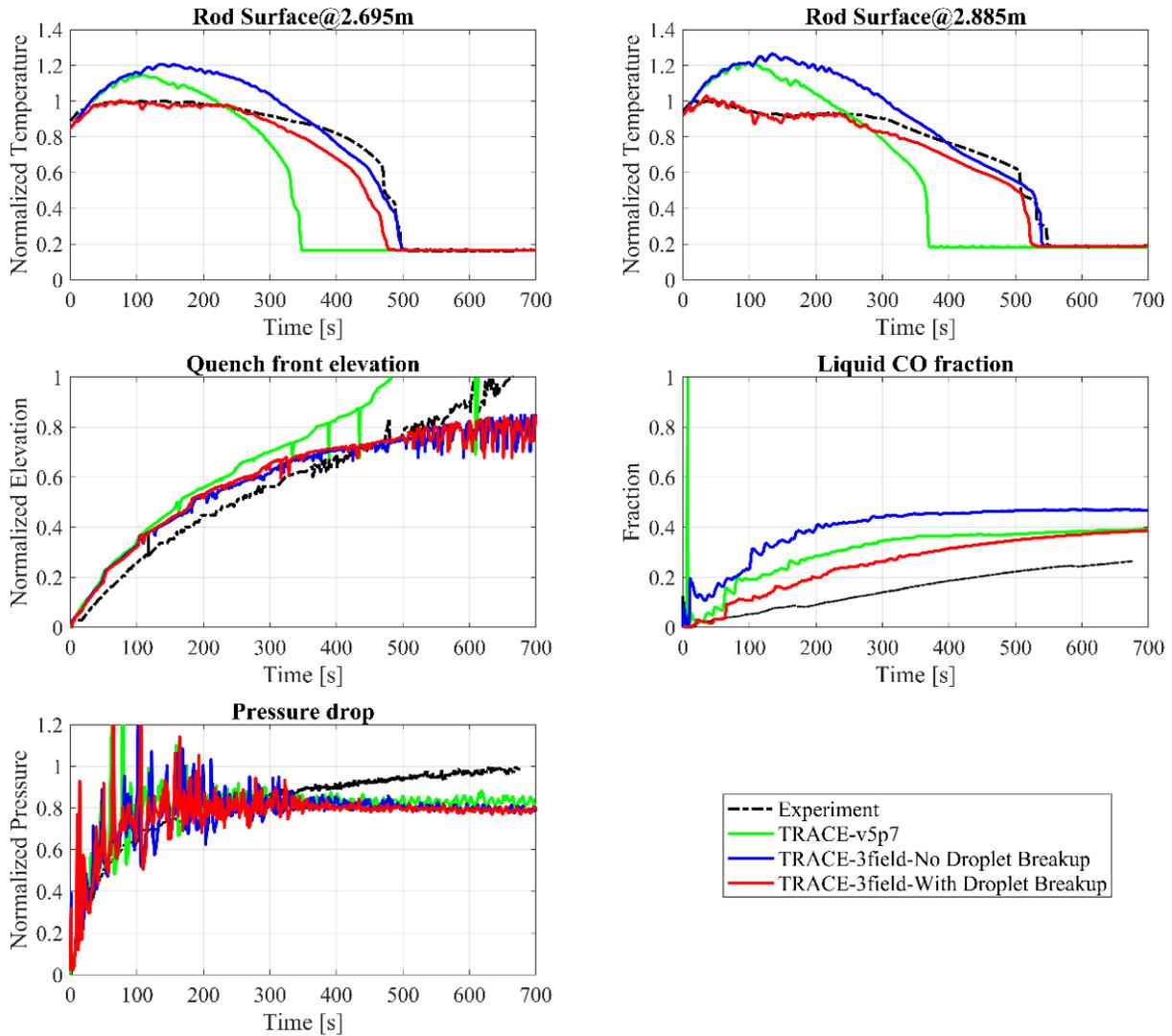


Figure 5-5 Evolution of RBHT Thermal Hydraulic Parameters During Reflood Test -9021.

5.2 Influence of Time Step

This section presents a sensitivity analysis of the time step on the prediction of rod surface temperature and quenching time during reflood. The simulations were conducted using TRACE 3F and TRACE 3F-DB to simulate each of the RBHT open tests, employing four different maximum time steps: 0.001, 0.003, 0.005, and 0.025 seconds. The simulations were performed using the same TRACE model. The sensitivity analysis results are presented through Figure 5-7 to Figure 5-15, which show the comparison of TRACE's prediction of the rod surface temperature to experimental measurements. The results indicate that increasing the time step delays the quenching time; with the effect being particularly pronounced for low reflood rate and low subcooling temperature conditions. The sensitivity of these operating conditions to the time step is significant, as even a slight increase in the time step from 0.003 to 0.005 seconds can greatly change the quenching time for up to 100 seconds. In contrast, increasing the time step to 0.025 seconds results in unrealistic behavior of the rod surface temperature and quenching time, although the TRACE code continues to run without crashing. The time step had no significant influence on the peak cladding temperature (PCT) predictions for the case 9021. For the same reflood rate but higher subcooling temperature, the time step had a minimal effect on the quenching time and PCT, as shown in Figure 5-8 for case 9026. However, increasing the time step slightly increased the PCT for TRACE 3F-DB calculations.

For the experimental conditions of a medium reflood rate (5.0 cm/s) and low subcooling temperature (10 K), such as in the case of 9005, the numerical time step has negligible influence on the results obtained using TRACE 3F, as shown in Figure 5-9. Nevertheless, increasing the time step for TRACE 3F-DB results in an increase in peak cladding temperature (PCT), although the quenching time is only slightly delayed by approximately 10 seconds, when the time step is increased from 0.001 to 0.025 seconds. However, for high reflood rates, such as 15 cm/s, and low subcooling temperatures (10 K), as seen in case 9015, the time step significantly affects the PCT predictions and quenching time, as demonstrated in Figure 5-10. Conversely, the results obtained using TRACE 3F are relatively insensitive to variations in the time step. Notably, the time step has no effect on the quenching time at higher subcooling temperatures, as illustrated in Figure 5-11 for case 9014, where an 80 K subcooling temperature was used. In this case, an increase in the time step only results in a slight increase in the PCT for TRACE 3F-DB results. The RBHT simulations have demonstrated that the time step effect is depending upon the reflood rate and subcooling temperature. However, this effect is primarily evident in the second half of the heated length, specifically downstream of the power peak location, as illustrated in Figure 5-12 to Figure 5-15. In this region, the complexity of the two-phase flow increases, and the droplet field and droplet breakup become more sensitive to variations in the time step. This sensitivity is most prominent for high reflood rates and low subcooling temperatures, as demonstrated in Figure 5-14 for the 9015 case. Conversely, the influence of the time step is minimal for low reflood rates and high subcooling temperatures. However, some variations in the peak cladding temperature are observed near the outlet of the test section, as indicated in Figure 5-13.

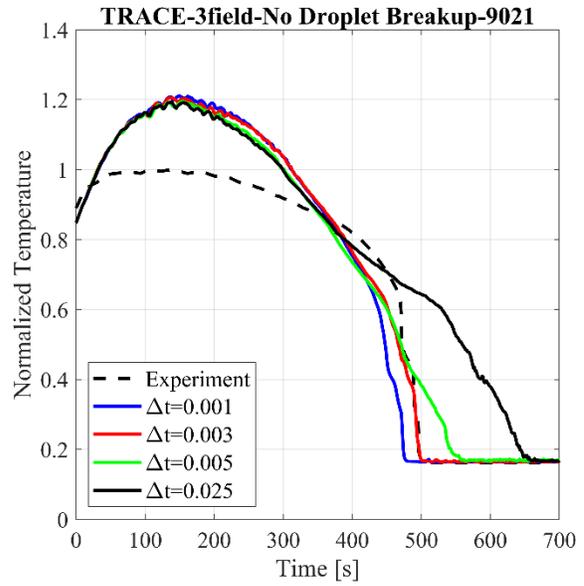
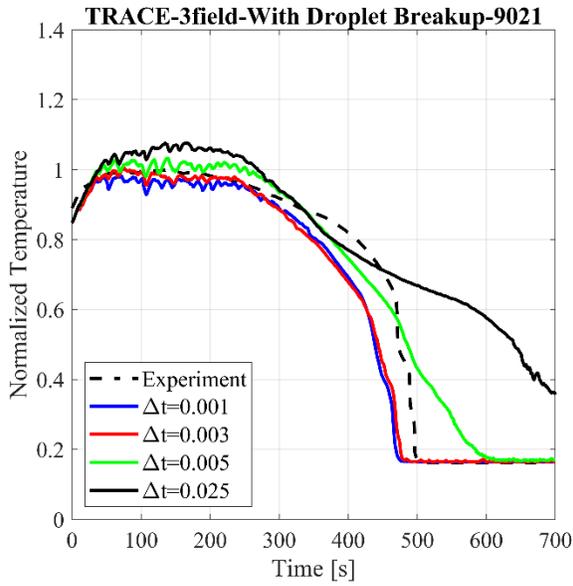


Figure 5-7 RBHT Rod Surface Temperature At 2.695 M For Low Reflood Rate and Low Subcooling Temperature Case (2.5 Cm/S, And 10 K).

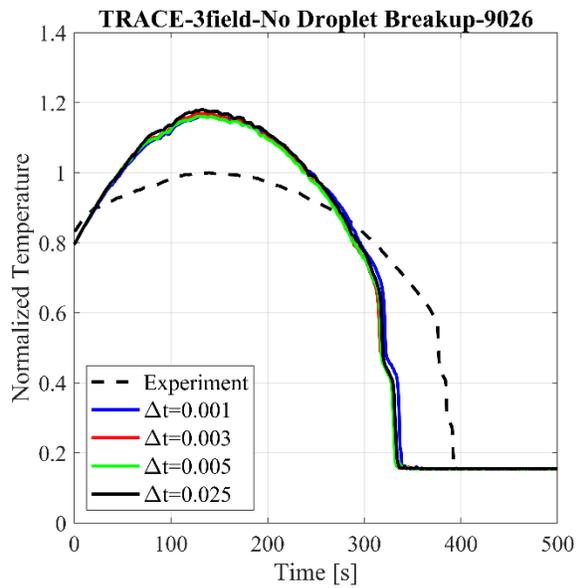
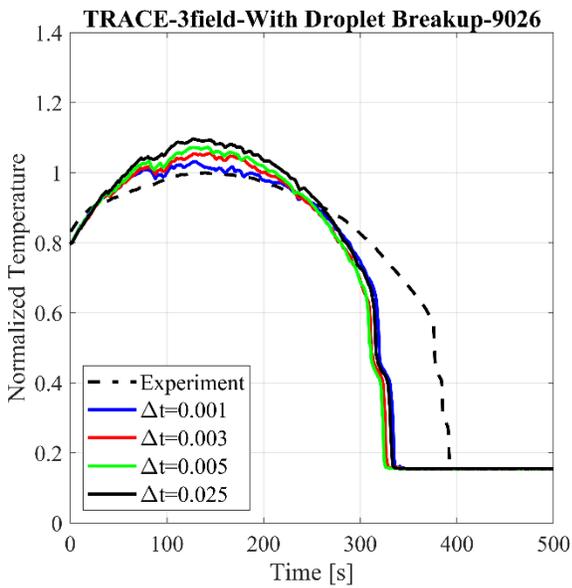


Figure 5-8 RBHT Rod Surface Temperature At 2.695 M For Low Reflood Rate and High Subcooling Temperature Case (2.5 Cm/S, And 80 K).

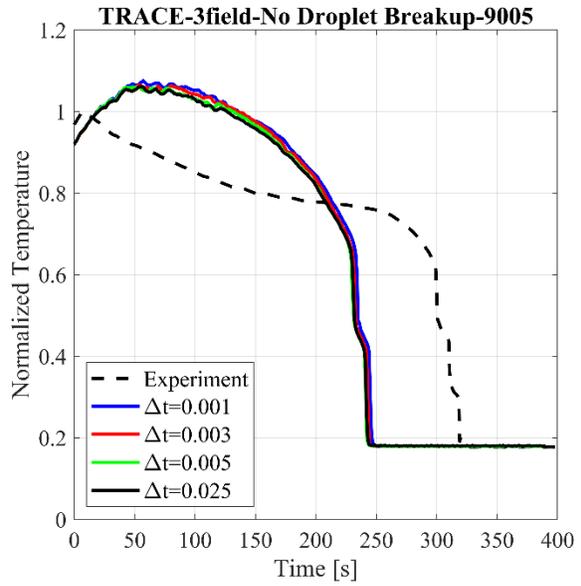
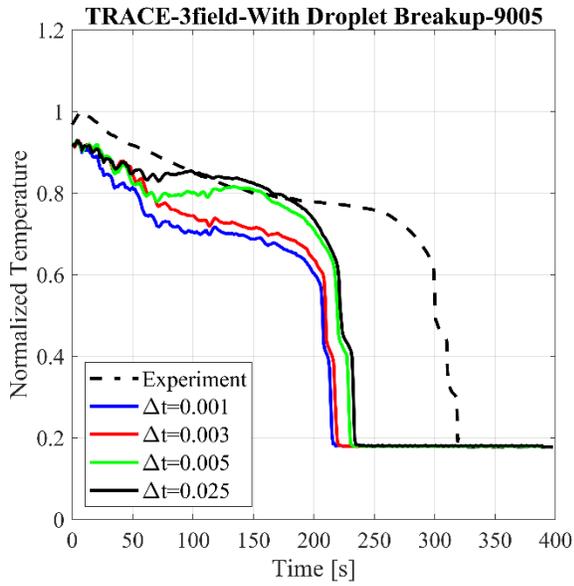


Figure 5-9 RBHT Rod Surface Temperature At 2.695 M For Medium Reflood Rate and Low Subcooling Temperature Case (5.0 Cm/S, And 10 K).

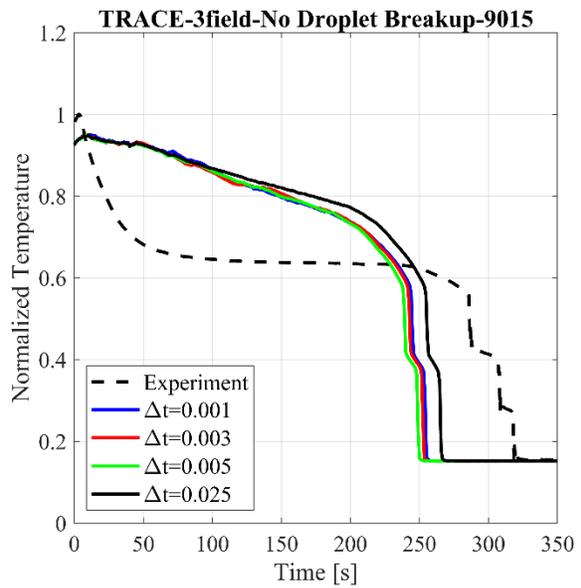
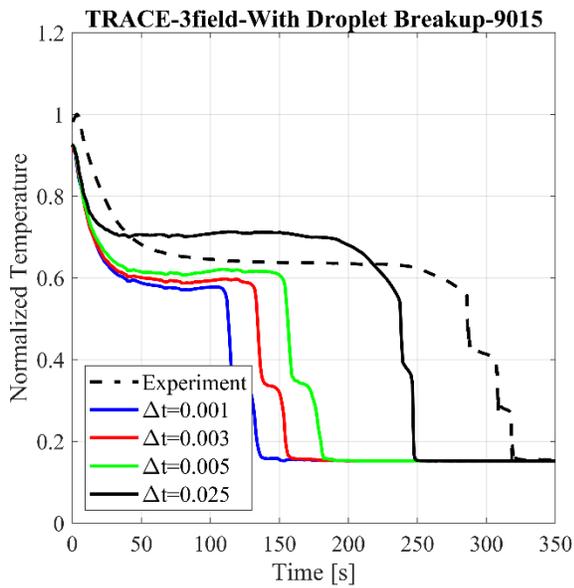


Figure 5-10 RBHT Rod Surface Temperature At 2.695 M For High Reflood Rate and Low Subcooling Temperature Case (15.0 Cm/S, And 10 K).

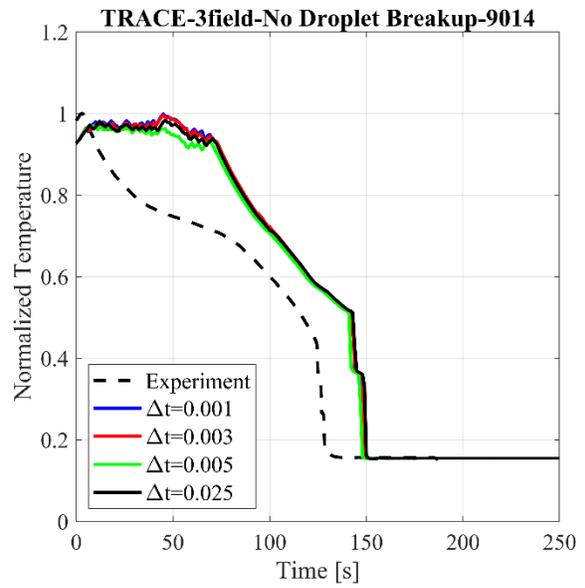
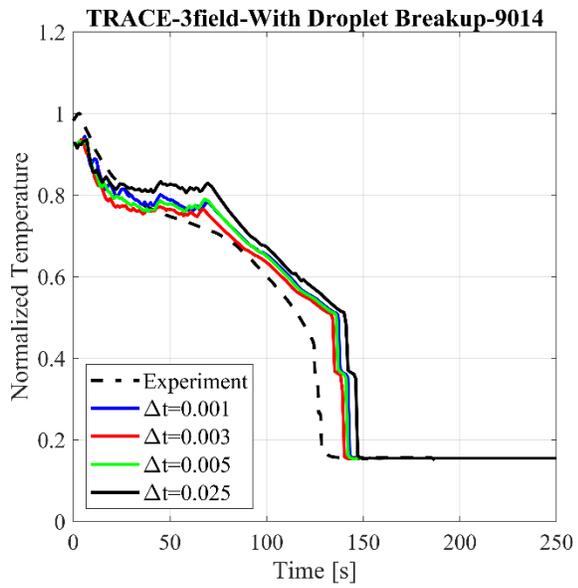


Figure 5-11 RBHT Rod Surface Temperature At 2.695 M For High Reflood Rate and High Subcooling Temperature Case (15.0 Cm/S, And 80 K).

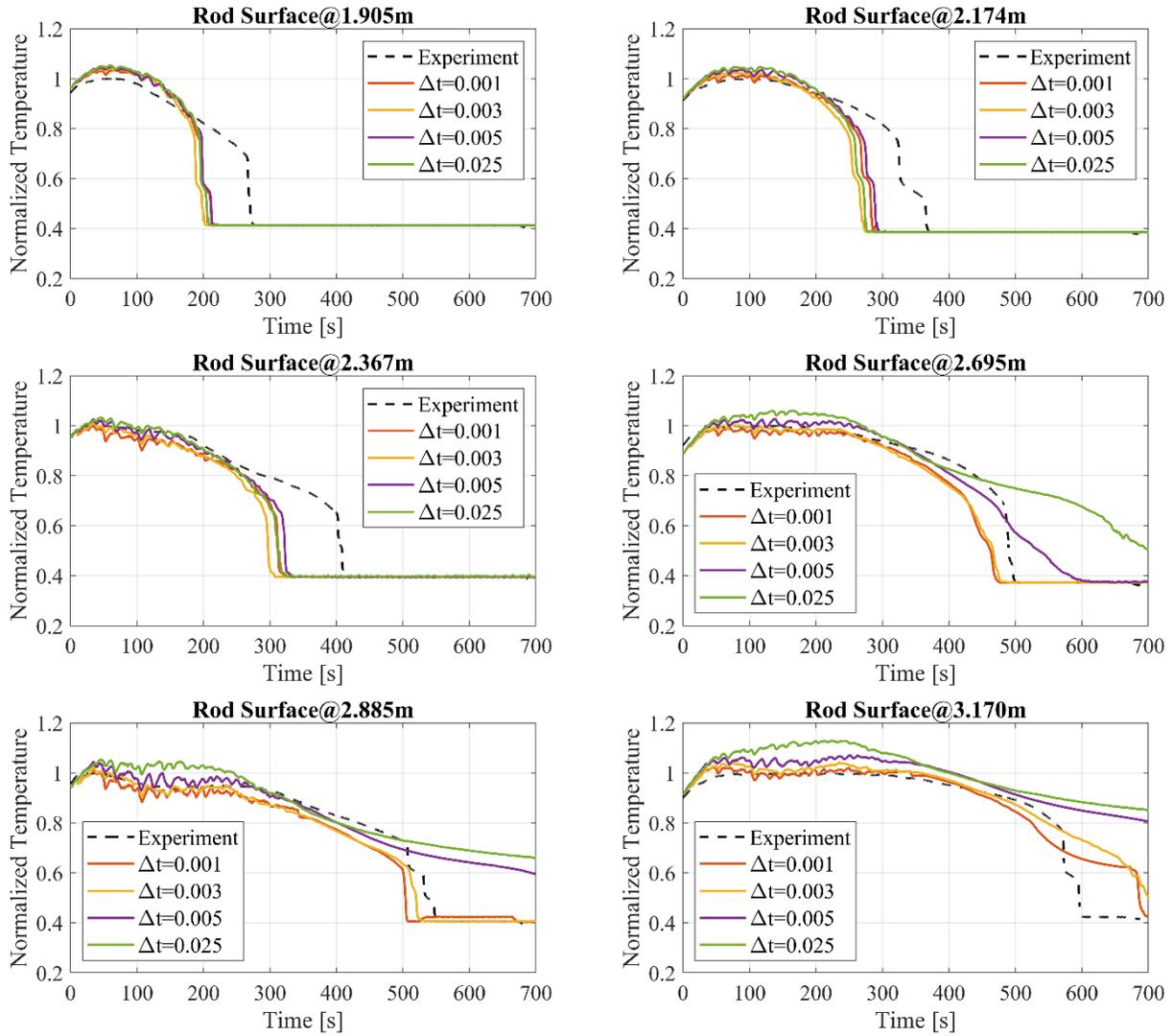


Figure 5-12 Influence of Time Step on The Axial Temperature Distribution For Test 9021 (2.5 Cm/S, And 10 K).

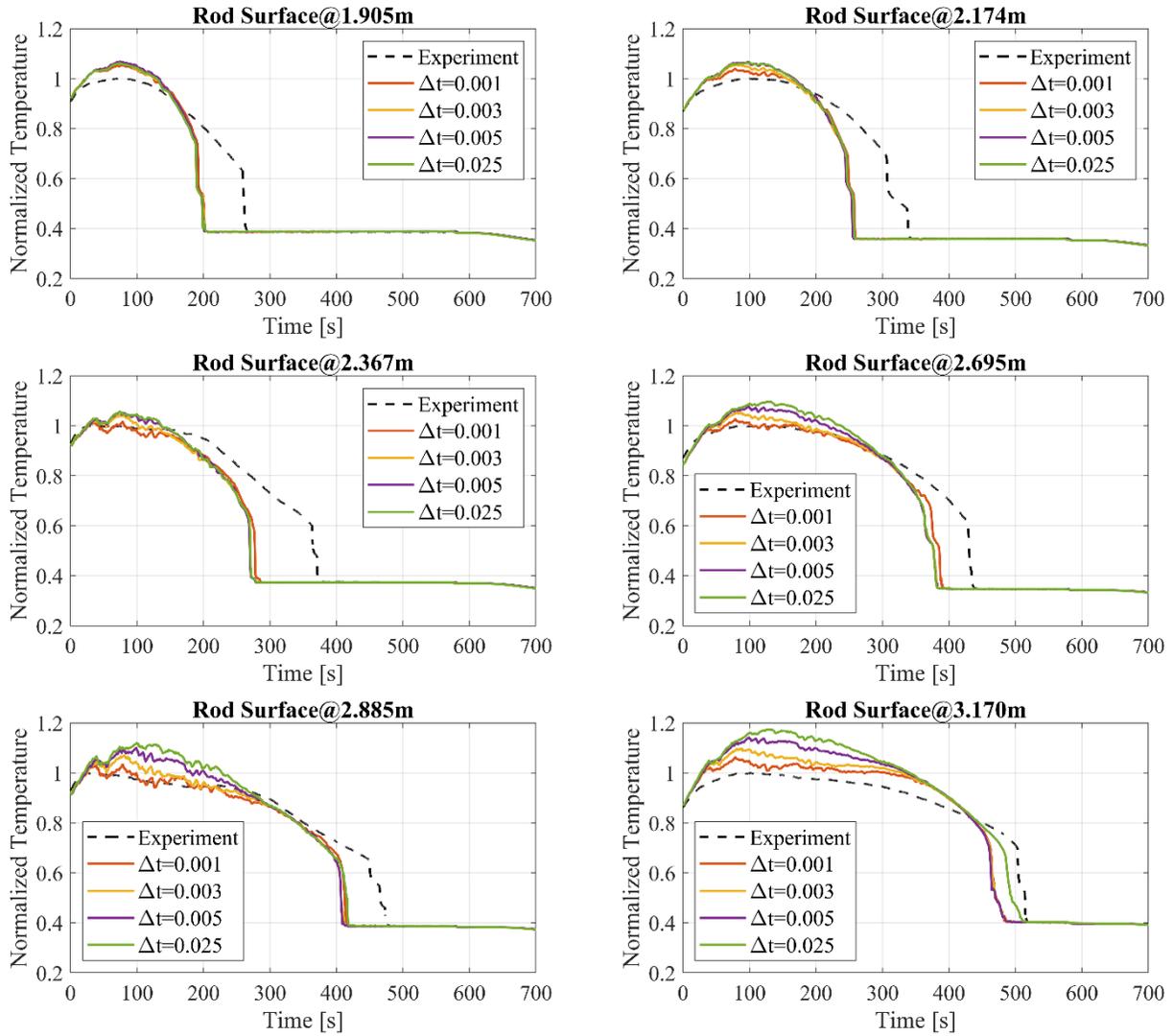


Figure 5-13 Influence of Time Step on The Axial Temperature Distribution For Test 9029 (2.5 Cm/S, And 47 K).

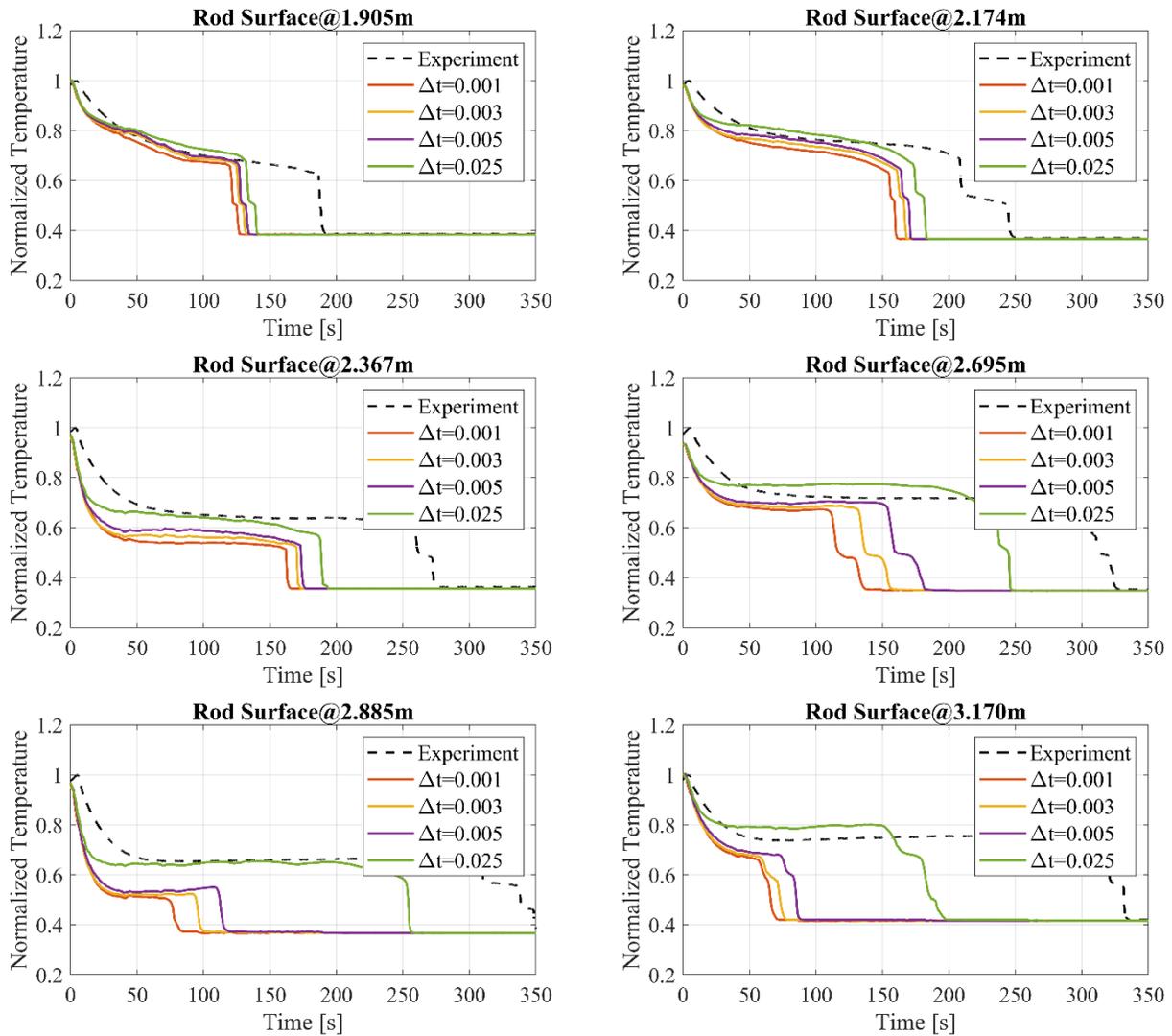


Figure 5-14 Influence of Time Step on The Axial Temperature Distribution For Test 9015 (15.0 Cm/S, And 10 K).

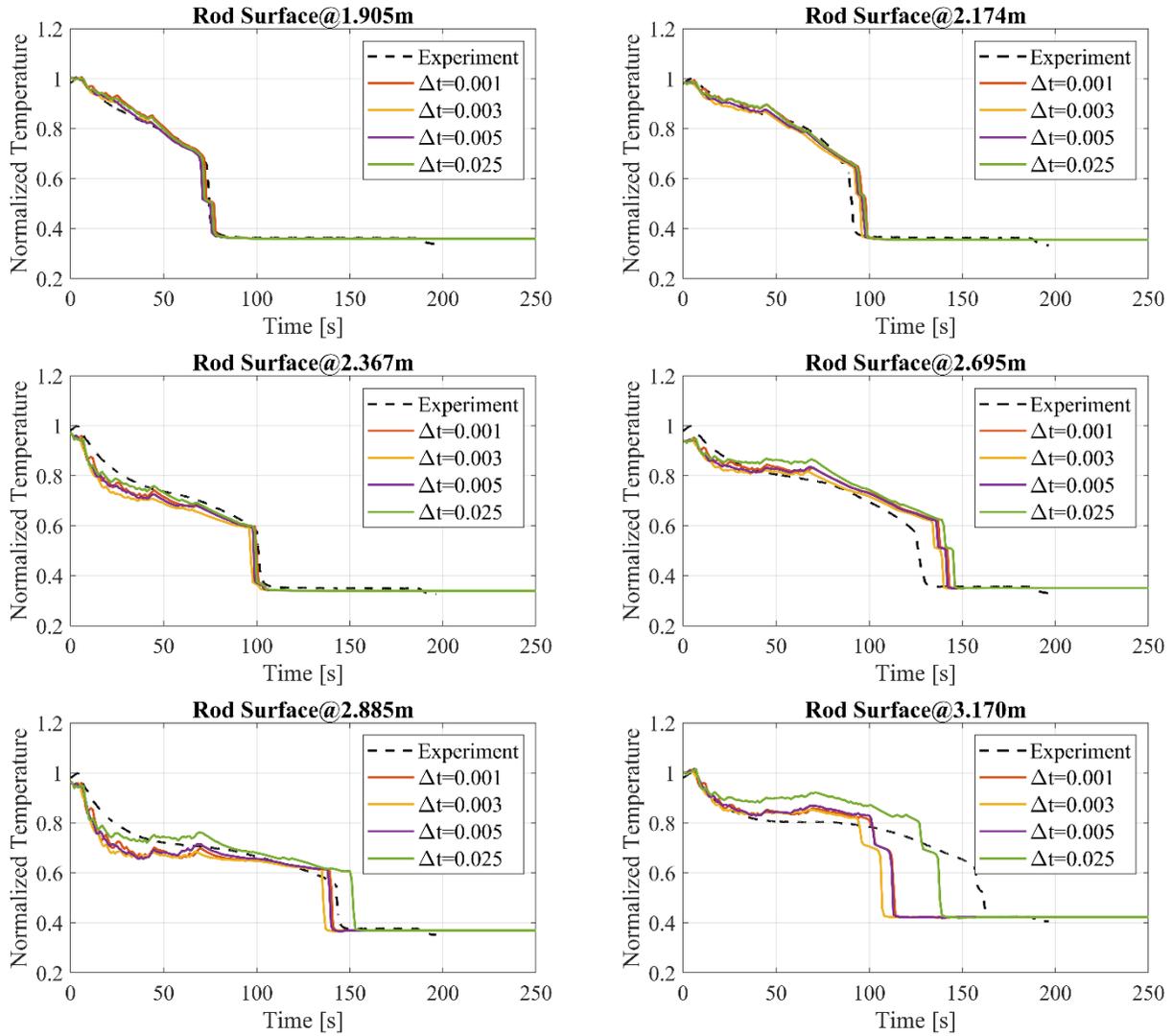


Figure 5-15 Influence of Time Step on The Axial Temperature Distribution For Test 9014 (15.0 Cm/S, And 80 K).

5.3 Effect of Numerical Solution Method

TRACE code implements two numerical solution methods to solve the fluid mass, momentum, and energy equations, namely the semi-implicit and Stability Enhancing Two-Step (SETS) methods [5]. The SETS method is the default option (NoSETS = 0) and has the advantage of avoiding Courant stability limit on time-step size, but it has disadvantage of relatively high numerical diffusion. On the other hand, the semi-implicit method (NoSETS = 1) has less numerical diffusion, but the time step size is limited by the Courant number. In this section, we examine the effect of the numerical solution method of the behavior of rod surface temperature and quenching time. To make a comparison, we selected a fixed time-step of 0.003 seconds for both solution options, and the results are presented in Figure 5-16 to Figure 5-18. The predictions of quenching time and rod surface temperature are similar for the two numerical methods, regardless of the reflood operation conditions.

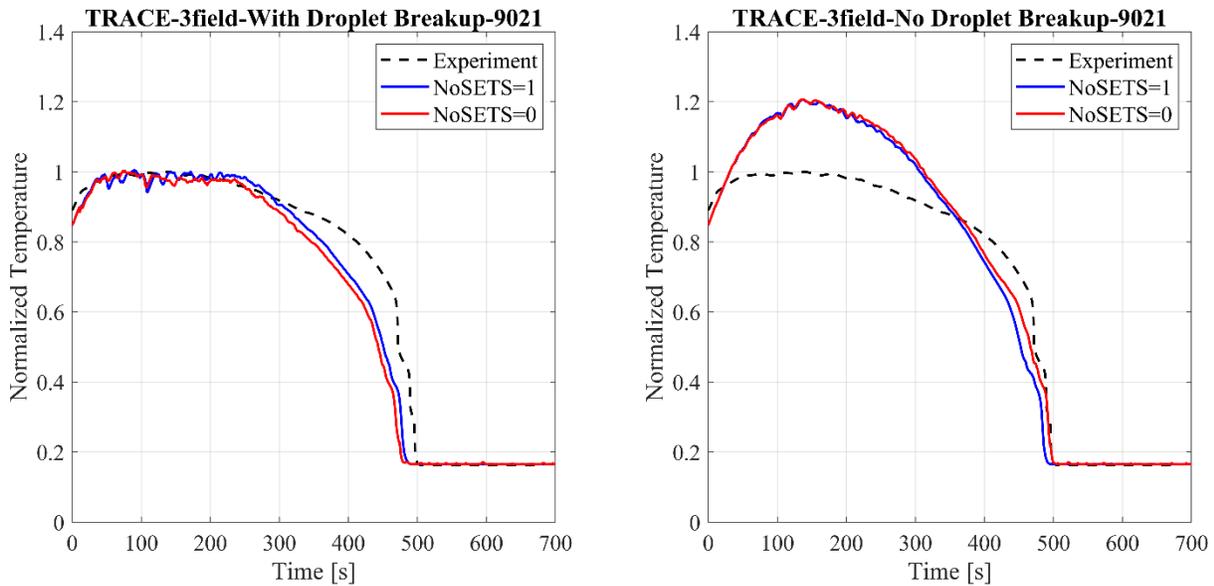


Figure 5-16 The Effect of The Numerical Scheme on The Rod Surface Temperature At 2.695 M For Low Reflood Rate and Low Subcooling Temperature Case (2.5 Cm/S, And 10 K).

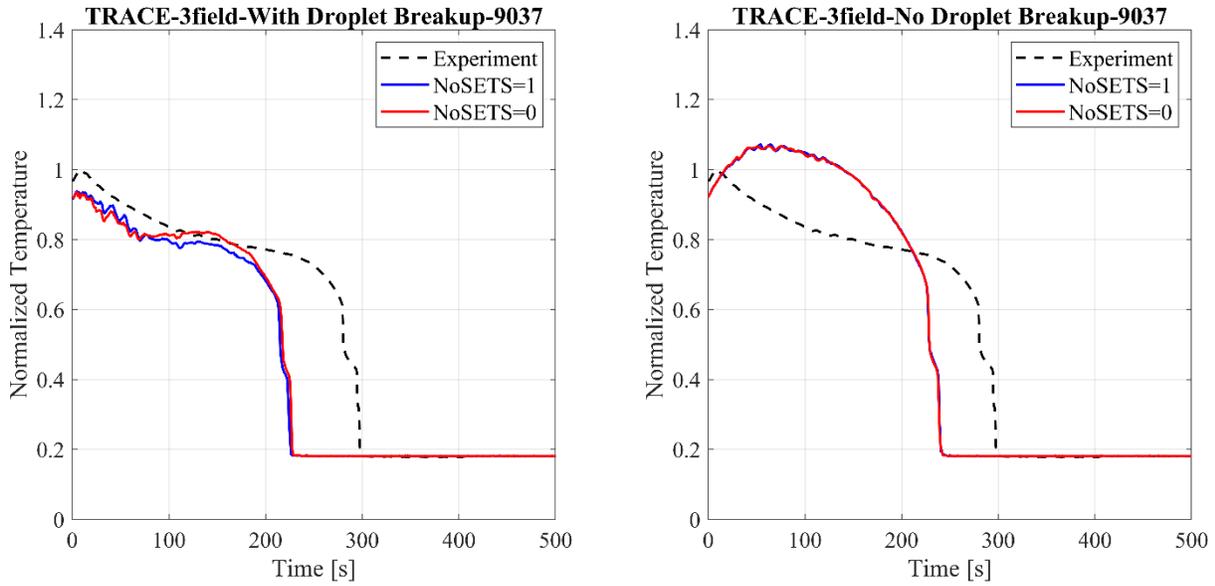


Figure 5-17 The Effect of The Numerical Scheme on The Rod Surface Temperature At 2.695 M For Medium Reflood Rate and Low Subcooling Temperature Case (5.0 Cm/S, And 10 K).

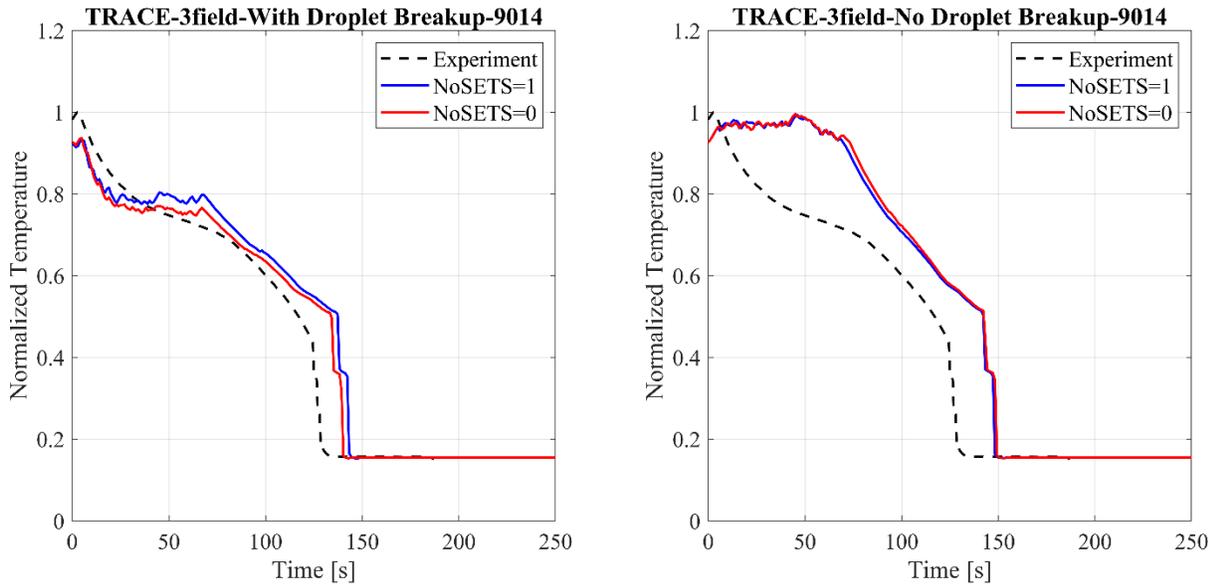


Figure 5-18 The Effect of The Numerical Scheme on The Rod Surface Temperature At 2.695 M For High Reflood Rate and High Subcooling Temperature Case (15.0 Cm/S, And 80 K).

6 CONCLUSION

This study evaluated the performance of three versions of TRACE (v5p7, 3F, and 3F-DB) in predicting the reflooding process during postulated LOCA scenarios. The analysis was based on the RBHT experimental tests with different reflood rates and inlet velocities. The spacer grids have a significant influence on the flow behavior inside the fuel assembly, particularly for two-phase flow regimes. The influence of the spacer grid droplet breakup models on the prediction of reflood phenomena is discussed in this study. The predicted results from the three different TRACE versions are compared against the RBHT experimental data. The results show that the droplet field and droplet breakup models significantly enhance interfacial heat and mass transfer. The results suggest that the droplet breakup model has a significant impact on the prediction of reflood phenomena, and it is crucial to include in simulations to improve accuracy. The results show that TRACE 3F and 3F-DB offer more accurate predictions compared to TRACE v5p7 in terms of quenching time and rod surface temperatures. However, all TRACE models tend to overpredict the liquid carryover fraction. The study also found that during very low reflood rates, the droplet field has a minor effect, and/or the generated droplets are small enough that cannot be captured with the current single group droplet field model.

The sensitivity analysis presented in this study demonstrated that the time step has a significant effect on the prediction of rod surface temperature and quenching time during reflood, particularly for low reflood rate and low subcooling temperature conditions. Increasing the time step delays the quenching time, and even a slight increase in the time step can greatly change the quenching time. However, increasing the time step to a certain extent results in unrealistic behavior of the rod surface temperature and quenching time. The time step had no significant influence on the peak cladding temperature predictions in some cases, while in others, increasing the time step slightly increased the PCT. The effect of the time step is most prominent in the second half of the heated length, downstream of the power peak location, where the complexity of the two-phase flow increases, and the droplet field and droplet breakup become more sensitive to variations in the time step. The influence of the time step is minimal for low reflood rates and high subcooling temperatures. Therefore, selecting an appropriate time step is important for accurate predictions of the rod surface temperature and quenching time during reflood simulations. Additionally, both numerical solution methods yield similar predictions for the quenching time a rod surface temperature, regardless of the reflood operation conditions. The accurate modeling of the reflooding process in BWRs and PWRs is highly important to ensure the safety of nuclear power plants.

7 REFERENCES

1. IAEA, Safety margins of operating reactors, Analysis of uncertainties and implications for decision making 2003.
2. Jin, Y., et al., Development of a droplet breakup model for dry spacer grid in the dispersed flow film boiling regime during reflood transients. *International Journal of Heat and Mass Transfer*, 2019. **143**: p. 118544.
3. Choi, T.S. and H.C. No, An improved RELAP5/MOD3.3 reflood model considering the effect of spacer grids. *Nuclear Engineering and Design*, 2012. **250**: p. 613-625.
4. Cheung, F.B. and S.M. Bajorek, Dynamics of droplet breakup through a grid spacer in a rod bundle. *Nuclear Engineering and Design*, 2011. **241**(1): p. 236-244.
5. Commission, U.S.N.R., TRACE V5.0 Patch 7 Theory Manual. 2022, Washington, DC: U.S. Nuclear Regulatory Commission: Office of Nuclear Regulatory Research.
6. OECD/NEA, RBHT Project Report 2022.
7. Koszela, Z., Assessment of RELAP5/MOD3.2.2 Gamma against ABB Atom 3×3-Rod Bundle Reflooding Tests. *Nuclear Engineering and Design*, 2003. **223**(1): p. 49-73.
8. Choi, T.S. and H.C. No, Improvement of the reflood model of RELAP5/MOD3.3 based on the assessments against FLECHT-SEASET tests. *Nuclear Engineering and Design*, 2010. **240**(4): p. 832-841.
9. Perret, G., I. Clifford, and H. Ferroukhi, Bias and uncertainty considerations for trace predictions of RBHT reflood experiments, in 19th international topical meeting on nuclear reactor thermal hydraulics (NURETH-19). 2019, American Nuclear Society (ANS): Brussels.
10. Sugimoto, J. and Y. Muraov, Effect of grid spacers on reflood heat transfer in PWR-LOCA. *journal of Nuclear Science and Technology*, 1984. **21**(2): p. 103-114.
11. Lee, S., et al., LDA in situ study of droplet hydrodynamics across grid spacers in PWR-LOCA reflood. 1983.
12. Lee, S.L., S. Cho, and H. Sheen, A study of droplet hydrodynamics across a grid spacer. 1984: Division of Accident Evaluation, Office of Nuclear Regulatory Research, US
13. Chiou, J., et al. Spacer grid heat transfer effects during reflood. in Joint NRC/ANS Meeting on Basic Thermal Hydraulic Mechanisms in LWR Analysis. 1982.
14. Nithianandan, C., J. Klingenfus, and S. Reilly, RELAP5 model to simulate the thermal-hydraulic effects of grid spacers and cladding rupture during reflood. 1995, US Nuclear Regulatory Commission (NRC), Washington, DC (United States). Div
15. Wachters, L.H.J. and N.A.J. Westerling, The heat transfer from a hot wall to impinging water drops in the spheroidal state. *Chemical Engineering Science*, 1966. **21**(11): p. 1047-1056.

16. Pederson, C.O., The Dynamics and Heat Transfer Characteristics of Water Droplets Impinging Upon a Heated Surface, in Department of Mechanical Engineering. 1967, Carnegie Mellon University.
17. Hamdan, K.S., D.-E. Kim, and S.-K. Moon, Droplets behavior impacting on a hot surface above the Leidenfrost temperature. *Annals of Nuclear Energy*, 2015. **80**: p. 338-347.
18. Paik, C., et al., Analysis of FLECHT-SEASET 163-rod blocked bundle data using COBRA-TF. 1985, Westinghouse Electric Corp., Pittsburgh, PA (USA).
19. Yao, S., L. Hochreiter, and K. Cai, Dynamics of droplets impacting on thin heated strips. 1988.
20. Paddock, M.D., Axial Photographic Technique for Droplet Size and Distribution of Two-Phase Dispersed-Annular Flow Through a Simulated Nuclear Reactor Grid, in Department of Mechanical Engineering. 1977, Wichita State University.
21. Rane, A. and S. Yao, Turbulent mist flow heat transfer in straight ducts. *ASME JOURNAL OF HEAT TRANSFER*, 1981. **103**: p. 679-684.
22. Senda, J., Experimental studies on the behavior of a small droplet impinging upon a hot surface. *ICLASS-82*, 1982. **397**.
23. Koszela, Z., Effects of spacer grids with mixing promoters on reflood heat transfer in a PWR LOCA. *Nuclear technology*, 1998. **123**(2): p. 156-165.
24. Cho, S., et al., Spacer grid effects during a reflood in an annulus flow channel. *Journal of nuclear science and technology*, 2007. **44**(7): p. 967-976.
25. In, W.-K., et al., Numerical computation of heat transfer enhancement of a PWR rod bundle with mixing vane spacers. *Nuclear Technology*, 2008. **161**(1): p. 69-79.
26. Ergun, S., L.E. Hochreiter, and J.H. Mahaffy, Modifications to COBRA-TF to model dispersed flow film boiling with two flow, four field Eulerian–Eulerian approach – Part 2. *Annals of Nuclear Energy*, 2008. **35**(9): p. 1671-1676.
27. Miller, D.J., Single-phase and two-phase grid-enhancement heat transfer in the reflood stage of a loss of coolant accident. 2012.
28. Lee, S., et al., Measurement of droplet dynamics across grid spacer in mist cooling of subchannel of PWR. 1984.
29. Akhtar, S. and A. Yule, Droplet impaction on a heated surface at high Weber numbers. *ILASS-Europe, Zurich*, 2001: p. 37.
30. Jin, Y., et al., Development of a new spacer grid pressure drop model in rod bundle for the post-dryout two-phase flow regime during reflood transients. *Nuclear Engineering and Design*, 2020. **368**: p. 110815.

31. Jin, Y., Investigation of Two-Phase Flow Thermal-Hydraulic Behavior in Rod Bundle during Reflood Transients Based on the RBHT Experimental Data. 2019: The Pennsylvania State University.
32. Hochreiter, L., et al., RBHT reflood heat transfer experiments data and analysis. University Park (PA): US Nuclear Regulatory Commission; 2012. 2012, NUREG/CR-6980.
33. Hochreiter, L., et al., Rod bundle heat transfer test facility test plan and design. NUREG CR-6975. US Nuclear Regulatory Commission, 2010.
34. OECD/NEA. Rod Bundle Heat transfer (RBHT) Project. 2019; Available from: https://www.oecd-nea.org/jcms/pl_25253/rod-bundle-heat-transfer-rbht-project.

BIBLIOGRAPHIC DATA SHEET

(See instructions on the reverse)

NUREG/IA-0543

2. TITLE AND SUBTITLE

Implementation of droplet breakup mode in TRACE to improve the prediction of reactor core reflood conditions

3. DATE REPORT PUBLISHED

MONTH	YEAR
November	2023

4. FIN OR GRANT NUMBER

5. AUTHOR(S)

Omar S. Al-Yahia*, Matthew Bernard**, Ivor Clifford*, Grégory Perret*, Stephen Bajorek**, Hakim Ferroukhi*

6. TYPE OF REPORT

Technical

7. PERIOD COVERED (Inclusive Dates)

8. PERFORMING ORGANIZATION - NAME AND ADDRESS (If NRC, provide Division, Office or Region, U. S. Nuclear Regulatory Commission, and mailing address; if contractor, provide name and mailing address.)

Paul Scherrer Institute, Laboratory for Reactor Physics and Thermal-Hydraulics
5232 Villigen PSI
Switzerland

9. SPONSORING ORGANIZATION - NAME AND ADDRESS (If NRC, type "Same as above", if contractor, provide NRC Division, Office or Region, U. S. Nuclear Regulatory Commission, and mailing address.)

Division of Systems Analysis
Office of the Nuclear Regulatory Research
U.S. Nuclear Regulatory Commission
Washington, D.C. 20555-0001

10. SUPPLEMENTARY NOTES

K. Tien, NRC Project Manager

11. ABSTRACT (200 words or less)

Reflood conditions exhibit complex two-phase flows in fuel assemblies featuring spacer grids. Spacer grids can shatter or split dispersed droplets thereby significantly reducing their diameters, increasing the local heat and mass interfacial transfer, and reducing peak cladding temperature (PCT). The diameter of dispersed droplets downstream of a spacer grid has been shown to be dependent on the Weber number of the incoming droplets and the spacer grid blockage ratio. In this work, a spacer grid droplet breakup model based on the droplet Weber number is implemented into the new three-field version of the U.S. Nuclear Regulatory Commission's TRACE code. The selected droplet break-up model can capture interfacial heat transfer enhancement observed in experimental data and is applicable to both mixing vane and egg-crate style spacer grids. The effect of the droplet breakup model on the three-field version of TRACE is assessed against recent RBHT (Rod Bundle Heat Transfer) experiments, for which TRACE was shown to overpredict the PCT for different initial and boundary conditions. When comparing the predictions of the base capability of TRACE and the three-field code with and without the spacer grid model, the new breakup model reduced the PCT predicted by TRACE by more than 100 K, which resulted in better-predicted PCTs and quenching times for the condition assessed

12. KEY WORDS/DESCRIPTORS (List words or phrases that will assist researchers in locating the report.)

TRACE, Droplet Entrainment, Reflood, Droplet Field, Spacer Grid

13. AVAILABILITY STATEMENT

unlimited

14. SECURITY CLASSIFICATION

(This Page)

unclassified

(This Report)

unclassified

15. NUMBER OF PAGES

16. PRICE



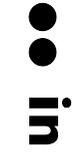
Federal Recycling Program



UNITED STATES
NUCLEAR REGULATORY COMMISSION
WASHINGTON, DC 20555-0001
OFFICIAL BUSINESS



@NRCgov



NUREG/IA-0543

Implementation of Droplet Breakup Mode in TRACE to Improve the Prediction of Reactor Core Reflood Conditions

November 2023